

Design, Spectroscopic Characterization, Electrical Conductivity and Molecular Modelling Studies of Biologically Puissant Co(II) and Ni(II) Complexes of N,N'-bis(furan-2-ylmethyl)benzene-1,2-dicarboxamide

Katabathini Narasimharao¹, Rayees Ahmad Shiekh^{2,*}, Maqsood Ahmad Malik^{1,*}, Musa A. Said², Zaheer Khan¹, Shaeel Ahmed Al-Thabaiti¹, Salman A. Khan¹

¹ Chemistry Department, Faculty of Science, King Abdulaziz University, P.O. Box 80203, Jeddah 21589, Saudi Arabia

² Department of Chemistry, Faculty of Science, Taibah University, PO Box 30002, Almadinah Almunawarra, Saudi Arabia

*E-mail: rayeeschem@gmail.com, maqsoodchem@gmail.com

Received: 14 December 2015 / Accepted: 24 March 2016 / Published: 7 July 2016

A series of N,N'-bis(furan-2-ylmethyl)benzene-1,2-dicarboxamide ligand (L) based metal complexes of general composition $M(L_2)X_2$ [where $M = Co(II)$, $Ni(II)$, and $L =$ ligand and $X = Cl^-$, CH_3COO^-] were synthesized by conventional and microwave irradiation synthesis methods. Both ligand and its metal complexes were characterized by elemental analysis, molar conductance, NMR (1H and ^{13}C), thermal analysis (TGA), infrared, UV-*vis*, mass spectral and molecular modelling studies. The elemental composition data revealed that the metal to ligand molar ratio is 1:2 in all synthesized complexes. The obtained spectroscopy results for synthesized complexes indicated that the ligand behaved as a bidentate ligand and agreed well with the proposed structures. The solid state electrical conductivity of the complexes was studied as a function of temperature, indicating the semiconducting nature of the metal complexes. In order to evaluate the antimicrobial activity of metal ions upon chelation, the newly synthesized ligand and its metal complexes were tested for their antibacterial and antifungal activities by the disk diffusion method. The antioxidant activity of the representative complex was evaluated by using 1,1-diphenyl-2-picrylhydrazyl (DPPH) radical scavenging method. The antimicrobial and antioxidant activity results indicated that all metal complexes have been found to be more effective than the ligand as the process of chelation dominantly affects the overall biological behavior of the compounds.

Keywords: N,N'-bis(furan-2-ylmethyl)benzene-1,2-dicarboxamide; Co(II), Ni(II) complexes; Antimicrobial activities

1. INTRODUCTION

The need of new compounds having enhanced activity against pathogenic bacteria and fungi is a need of present time because of growing microbial resistance to currently existed antibiotics [1]. The most spectacular advances in medicinal chemistry have been made when macrocyclic compounds played an important role in regulating biological activities. Transition metal complexes are among the most extensively studied coordination compounds in recent years because they are becoming progressively significant as biochemical, analytical and antimicrobial reagents [1,2]. The coordinated complexes containing metal ions are active in many biological processes and showed immense biological activity as allied with certain metal-protein. The coordinated metal complexes, which can contribute to oxygen transport, electronic transfer reactions or the storage of ions [3,4] has been generated massive interest [5]. Metal based drugs have achieved much significance in medicinal field and has been serving as medicines for the treatment of diabetes, cancer, anti-inflammatory and cardiovascular diseases [6-8]. In numerous biological processes metal chelation is involved in which the coordination can take place between an extensive array of ligands and different metal ion [9]. The significance of the coordination chemistry of tailored bioligands has gained much interest and widespread investigations has been reported for the potential biological activities of transition metal complexes [10,11]. During the past decade, there has been a growing interest in the synthesis of multidentate ligands which are illustrated for quadridentate ligands and their complexes. These days a variety of approaches are accessible for design and development of molecular systems which are biologically and medically has an importance [12-14]. Attempts have been made to design and develop the drugs based on metal and pyridine molecular devices [15,16]. It was reported that these drugs shown infiltration influence through pathogenic cell membranes and also have fondness for the pathogenic genetic material (DNA or RNA) [17,18].

Recently, synthetic and structural features of numerous transition metal complexes of NO and NS donor systems have been reported [19-22]. The structural properties and biological application of metal complexes vary by changing the ligands or metal ions. The fluctuation in biological activities of Cu(II) complexes were well documented [23,24]. The design and development of new ligands and their transition metal complexes may provide additional alternatives for the treatment of superficial fungal and bacterial infections, and may assist to conquer the restraints of existing treatments. By complexing these versatile ligands with different type of metals would make these ligands more potent compounds against microbes with broad spectrum. Numerous transition metal ions in living systems function as carriers or enzymes in a macrocyclic ligand environment and the metal is generally binds in a macrocyclic by means of conformational arrangement of the protein [29-31]. Metal complexes preparation has been the focus because of enhanced biological activities of the corresponding drug metal complexes. The essential target of the present work deals with synthesis, spectroscopic characterization, biological evaluation and antioxidant studies of N,N'-bis(furan-2-ylmethyl)benzene-1,2-dicarboxamide ligand based Co(II), Ni(II) complexes by conventional and microwave irradiation synthesis methods.

2. EXPERIMENTAL

2.1. Materials

All the chemicals, metal salts and solvents used in this investigation were of analytical reagent grade. Phthalic acid and furfurylamine were purchased from Merck (Germany) and were used as received. Metal salts [Cobalt(II) and Nickel(II) chloride/acetate] were purchased from Aldrich (USA) and used without further purification. All solvents used were of standard/spectroscopic grade were acquired commercially and utilized with no additional purification.

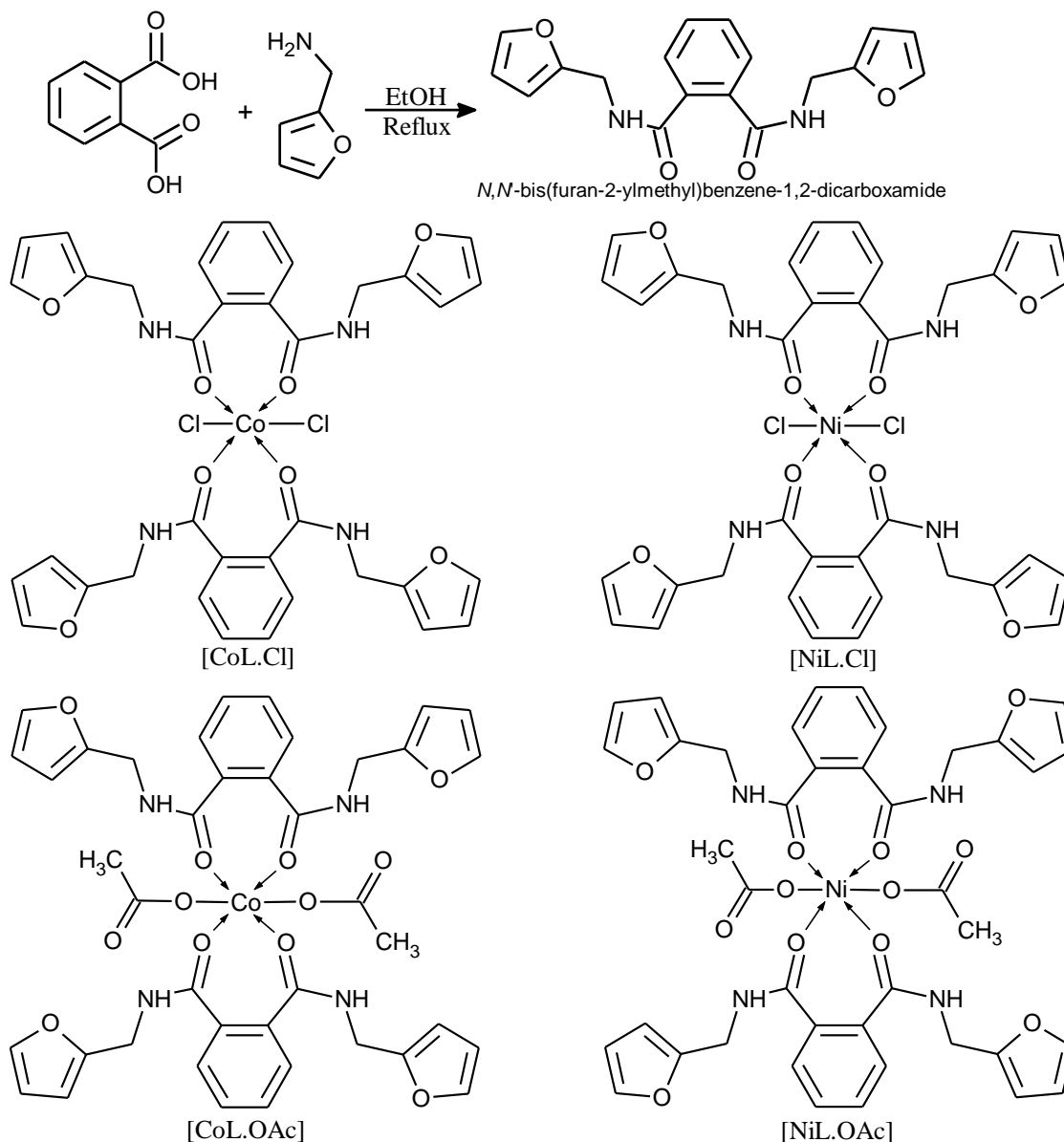
2.2. Preparation of the Ligand (*N,N'*-bis(furan-2-ylmethyl)benzene-1,2-dicarboxamide):

Conventional method: Furfuryl amine (2.44 g, 20 mmol) and phthalic acid (1.66 g, 10 mmol) were dissolved in 10 ml of ethanol separately. Both solutions were poured into a schlenk flask connected with a condenser and placed in an oil bath. The solution mixture was heated very slowly and was refluxed for 6 h under constant stirring. Then the reaction mixture was allowed to cool at room temperature and the obtained precipitate was filtered. The precipitate was then washed several times by methanol followed by diethyl ether and was recrystallized from methanol. This synthesized material was further dried in an electric oven at 50-60 °C (yield; 70-75%). *Microwave method:* The reaction mixture containing calculated amounts of phthalic acid and furfuryl amine was irradiated in the microwave oven (power 150 W) by mixing the reactants with 4 mL of dry ethanol. The synthesis process was completed in a short time (4 min) with excellent yields (90-95%). The resulting product was filtered and recrystallized with ethanol, finally the acquired product was dried under reduced pressure over anhydrous CaCl₂ in a desiccator. The outline synthesis of ligand is shown in Scheme 1. mp. 180 °C, ¹³C NMR (DMSO-d₆) δ (ppm): 160.0 (C-N), 156.62, 148.21, 135.63, 129.14, (Ar-C); ESI MS (m/z) 324 [M]⁺, 325 [M+1]⁺. Elem anal calcd C (66.60) H (4.93) N (8.63) O (19.73) %; found C 66.72, H 4.94, N 8.64, O 19.75.

2.3. Preparation of the metal complexes

Conventional method: The metal complexes; cobalt(II) complexes (LM₁ (metal chloride) and LM₃ (metal acetate) and nickel (II) complexes (LM₂ (metal chloride) and LM₄ (metal acetate) (Scheme 1) were synthesized in a schlenk flask by mixing 50 ml ethanolic solution of respective metal salt (Co(II), Ni(II) chloride/acetate) and 50 ml ethanolic solution of above synthesized ligand (L) in a 1:2 (metal/ligand) ratio. The reaction mixture was heated slowly by means of conventional electric heating and refluxed for 5-6 h under constant stirring. A resulting coloured product obtained was cooled at room temperature and the precipitated complex was filtered, washed several times with petroleum ether and recrystallized with ethanol and dried under reduced pressure over anhydrous CaCl₂ in a desiccator. The synthesised metal complexes were also dried in an electric oven at 50-60 °C (yield: 50-60%). *Microwave method:* The synthesized ligand and respective metal salts were mixed in 1:2 (metal: ligand) ratio and reaction mixture was irradiated in microwave oven (150 W) by taking 5 mL of dry

ethanol as a solvent. The reaction was completed in very short time (5 min) with excellent yields. The condensation product was kept at room temperature for few minutes. Finally the colored reaction product was filtered, thoroughly washed with ether and recrystallized with ethanol and dried under reduced pressure over anhydrous CaCl_2 .



Scheme 1. Synthesis of Ligand and its metal complexes (LM_1 - LM_4)

2.4. Analytical and physical measurements

The melting point of all synthesized compounds was determined by Metrex melting point apparatus and the results are uncorrected. Microanalysis of ligand and its metal complexes was performed on Heraeus Vario EL III analyzer. Bruker Tensor II FT-IR Spectrometer was used to obtain FTIR spectra of synthesized compounds reported in this present study. Proton NMR (^1H NMR) and

Carbon-13 NMR (^{13}C NMR) spectra of the ligand and its metal complexes were recorded in $\text{DMSO-d}_6/\text{CDCl}_3$ by employing tetramethylsilane (TMS) as internal standard on Bruker AVANCE DPX-600 spectrometer. The electronic absorption spectra of the ligand and its metal complexes were recorded by using Shimadzu UV-3600 UV-VIS-NIR Spectrophotometer using DMSO as solvent. Mass spectra of the ligand and its metal complexes were recorded by Bruker (esquire 3000-00037) mass spectrometer. Under nitrogen atmosphere the thermal analysis (TG/DTA) study was carried out by SII Ex Star 6000 TG/DTA 6300 instrument. Guoy's method was employed to measure the magnetic susceptibility at room temperature. Reaction progress and the purity of the synthesized compounds was examined by TLC performed on silica gel plates. The powdered complex was palletized in a steel disk of specific diameter under pressure 4 tons cm^{-2} with the help of hydraulic press. The pellets obtained were of an area 1.60 cm^2 with 1 mm thickness, and were hard and crack free. These pellets were coated carefully with silver paste to make good electrical contacts between surfaces and the electrodes. The conductivity was measured on solid state electrometer within the temperature range 308-438 K. The physical and spectroscopic data is given in the respective tables. Microwave method happened to be the efficient route for the synthesis of ligand (L) and its metal complexes (LM1 to LM4) with higher yields and high purity of the product in less reaction time (Table 1).

Table 1. Comparison between microwave and conventional electrical heating method.

Compound		Yield (%)		Solvent (mL)		Time	
		CHM*	MW [#]	CHM	MW	CHM (h)	MM(min)
Ligand	L	80	94	100	2	7	3
$[\text{CoL}_2\text{Cl}_2]$	LM₁	74	88	40	4	5	5
$[\text{NiL}_2\text{Cl}_2]$	LM₂	78	85	40	4	5	5
$[\text{CoL}_2(\text{CH}_3\text{COO})_2]$	LM₃	74	87	40	3	5	5
]						
$[\text{NiL}_2(\text{CH}_3\text{COO})_2]$	LM₄	71	84	40	3	6	6
]						

*CHM: Conventional heating method; [#]MW: Microwave

2.5. Molecular modelling studies

The 3D molecular modelling of the ligand (L) (Fig. 1) and its metal complexes (Fig 2 and 3) was carried out by using Chem Bio 3D Ultra (14.1 version) graphical software. Chem Bio 3D Ultra is a graphical program that provides speedy structure building, molecular display and geometry optimization with minimum energy. The ligand and its metal complexes were modelled by Chem Bio 3D Ultra after a number of cycles of energy minimization and correct stereochemistry was guaranteed through the amendment and manipulation of the molecular coordinates to acquire reasonable low energy molecular geometries. The optimized geometric parameters like bond lengths and bond angles of ligand and its metal complexes.

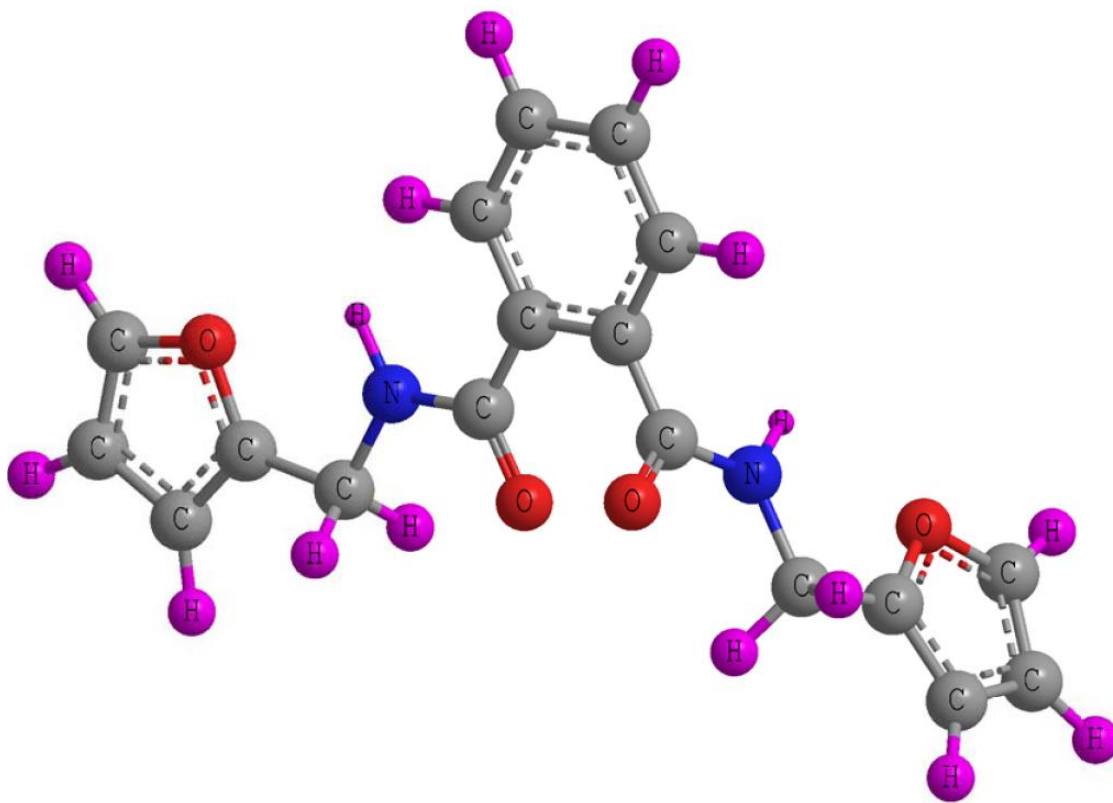


Figure 1. Geometry optimized structure of Ligand (L).

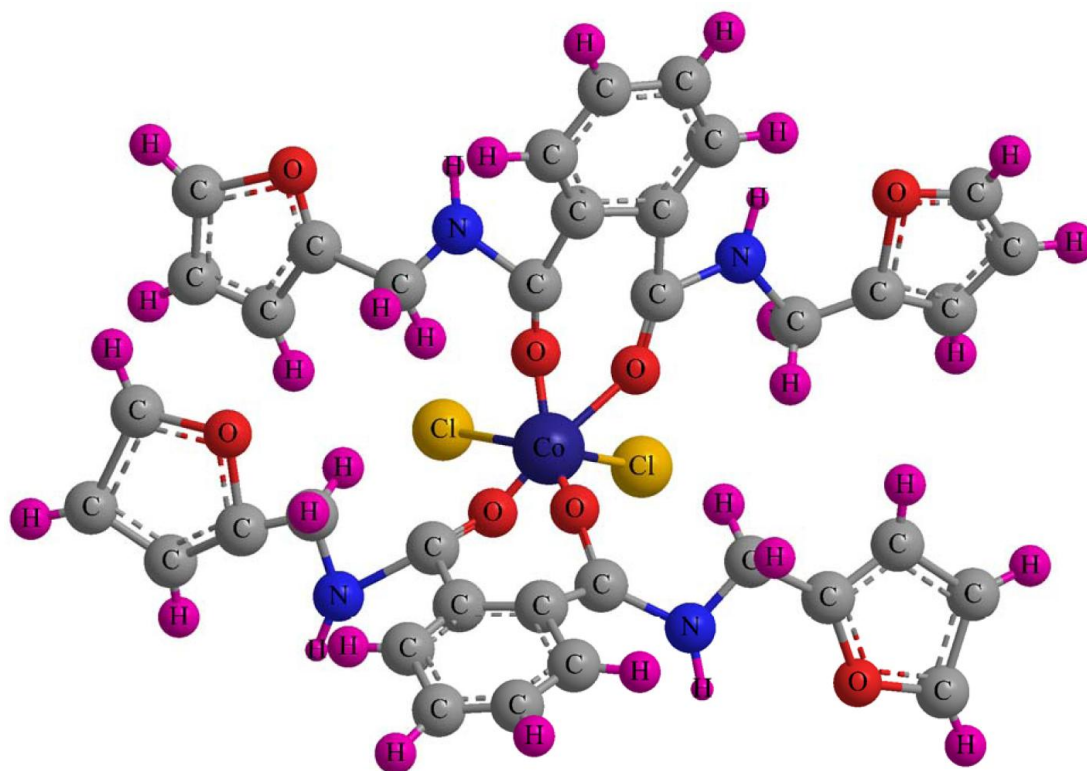


Figure 2. Geometry optimized structure of $[CoL_2Cl_2]$ metal complex.

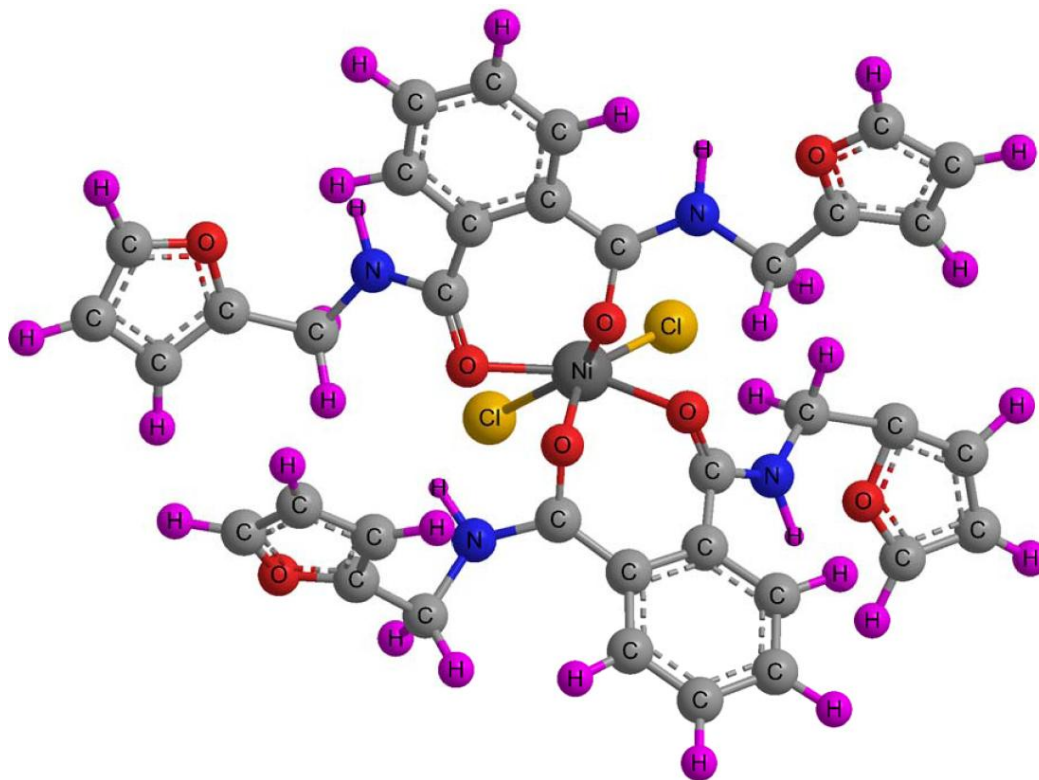


Figure 3. Geometry optimized structure of $[\text{NiL}_2\text{Cl}_2]$ metal complex.

2.6. Antimicrobial studies

The newly synthesized compounds (ligand and its metal complexes) were tested for their *in vitro* antimicrobial activity against the Gram-positive bacteria (*Staphylococcus aureus*, *Streptococcus pyogenes*), Gram-negative bacteria (*Escherichia coli*, *Klebsiella pneumoniae*) by disk diffusion method, using agar nutrient as the medium and Ampicillin as control. The antifungal activity was carried out against different fungal species like *Candida albicans*, *Candida glabrata*, *Candida tropicalis* and *Candida krusei* by disk diffusion method using potato dextrose agar as medium and Fluconazole as a control. The synthesized compounds were dissolved in DMSO to get stock solutions and in addition the stock solutions of the compounds were diluted by required volumes of freshly distilled DMSO to get different concentrations (100 , 75 , 50 , and $25 \mu\text{g mL}^{-1}$) of the synthesized compounds.

2.7. Antibacterial screening

The *in vitro* antibacterial screening effects of the investigated compounds were tested against *Staphylococcus aureus*, *Streptococcus pyogenes*, *Escherichia coli*, *Klebsiella pneumoniae* bacterial strains by disk diffusion method. Ampicillin ($30 \mu\text{g}$) was used as positive control, while the disc poured in DMSO was used as negative control. Muller-Hinton agar plates with final concentration of 100 , 75 , 50 and $25 \mu\text{g mL}^{-1}$ of synthesized compounds (ligand and its Co(II), Ni(II) metal complexes)

were vaccinated with standardized inoculums of test strains of bacteria (McFarland standard 0.5). Standard inoculums (McFarland standards) were spread onto the surface of sterile agar plates. A good quality Whatman filter paper was used for preparing a disc with 10-mm diameter. The sterile discs earlier drenched in a known concentration of the test compounds were placed in the nutrient agar medium. The plates were reserved at 5 °C for 1 h and then transferred to an incubator for incubation maintained at 36 °C for 24 h. On the other hand, a control plate of Muller-Hinton agar lacking the test compound was incubated with test strain of bacteria and kept for incubation at the same conditions. The susceptibility was measured on the basis of diameter of the zone of inhibition against Gram-positive and Gram-negative strains of bacteria. Zone of inhibition was measured and compared with the control strains. Broth micro dilution method was adopted for the determination of minimum inhibition concentration (MIC). The cultures of the bacterial strains were nurtured for 24 h at 37 °C and the growth was examined visibly and spectrophotometrically. The lowest concentration (highest dilution) necessitated to apprehend the growth of bacteria was considered as MIC. The experiments were carried out in triplicate and the standard values were computed for antibacterial activity.

2.8. Antifungal screening

The antifungal activity was carried out against *Candida albicans*, *Candida glabrata*, *Candida tropicalis* and *Candida krusei* fungal strains by disk diffusion method using potato dextrose agar as medium. Potato dextrose agar plates containing final concentration of 100, 75, 50 and 25 $\mu\text{g mL}^{-1}$ of ligand and its metal complexes were inoculated with 100 μL of 7 days old spore suspension of each fungal culture (108 spore/mL). The compounds dissolved in DMSO were soaked in filter paper disc of 10 mm diameter. These discs were kept for incubation at 32 °C for about 48 h and the diameter of inhibition zone around each disc was measured. A control potato dextrose agar plate exclusive of test compounds was reserved for incubation with its test strains of tested fungal species at similar conditions.

The MIC value of synthesized compounds was determined by serial dilution method. Immediately after the 48 h incubation period completes, the MIC of each test compound was noted as the minimum concentration of the compound with no observable growth of the fungal species. All the experiments were performed in triplicate and the observed average values were computed for antifungal activity. The lowest concentration of each test compound with no evident growth of test fungal species was accounted as MIC for their respective strains. On observing the blank tests, DMSO used for the preparation of the test solution does not have an effect on the test organisms. The results were compared with fluconazole for fungal strains as positive control.

2.9. Antioxidant activity

Antioxidant activity of the synthesized compounds was determined by DPPH free radical scavenging effect [35]. DPPH is one of the few stable and commercially available organic nitrogen radicals. DPPH radicals are considered as a representative method for the preliminary screening of

compounds able to scavenge activated oxygen species, since they are more stable and easier to handle than oxygen free radicals. The DPPH assay is considered as a standard assay in antioxidant activity investigations that provides a fast method for screening the radical scavenging activity of specific compounds or extracts [36]. It is considered as a stable free radical that can accept hydrogen radical or electron and becomes a stable diamagnetic molecule. DPPH shows a strong absorption band at 517 nm because of odd electron. By serial dilutions different concentrations (25, 50 and 75 μg) of samples were prepared in DMSO and 3 ml of DPPH solution was added and shaken vigorously for about 2-3 min, then incubated in a dark room for 30 min at room temperature. Butylated hydroxyanisole (BHA) used as the reference or positive control was taken in different test tubes. A blank DPPH solution was used for the baseline correction because the odd electron in the DPPH gave a strong absorption maximum at 517 nm (by using a Shimadzu UV-1601 spectrophotometer). After incubation, the absorbance values of each solution were measured at 517 nm and there was a change (decrease) in the absorbance values indicating that the complexes showed moderate free radical scavenging activity. The radical scavenging ability can be calculated according to the following equation and the results were compared with standard control.

$$\text{Scavenging Activity (\%)} = \frac{A_{\text{control}} - A_{\text{sample}}}{A_{\text{blank}}} \times 100$$

3. RESULTS AND DISCUSSION

Synthesis of the ligand and its metal complexes via microwave irradiation method is easier, convenient, and faster. Microwave method offered high yields of all the products compared to conventional heating method. All the metal complexes are colored solids and stable towards air and moisture at room temperature. They decomposed upon heating at high temperature, highly soluble in common non-polar organic solvents.

Table 2. Physical and analytical data of the ligand (L) and its complexes (LM₁-LM₄).

Compound	Color	MC*	M.P. (°C)	Mol. Wt % Found (Cal.)	Elemental analysis (%)				
					M	C	H	N	O
L	white		180	324.34 (325.40)		66.60 (66.62)	4.93 (4.94)	8.63 (8.64)	19.73 (19.75)
LM ₁	Green	12	>300	778.61 (779.15)	7.56 (7.59)	27.74 (27.79)	2.05 (2.08)	3.59 (3.61)	8.21 (8.23)
LM ₂	Royal blue	14	>300	778.37 (778.39)	7.54 (7.56)	27.75 (27.78)	2.05 (2.07)	3.59 (3.60)	8.22 (8.25)
LM ₃	Mauve pink	16	>300	825.61 (825.63)	7.13 (7.15)	31.97 (31.99)	2.30 (2.32)	3.39 (3.41)	15.50 (15.53)
LM ₄	Light green	18	>300	825.37 (825.40)	7.11 (7.15)	31.98 (32.00)	2.30 (2.34)	3.39 (3.42)	15.50 (15.52)

*Molar conductance: Λm ($\Omega^{-1}\text{cm}^2\text{mol}^{-1}$)

L= C₁₈H₁₆O₄N₂

The physical properties and analytical data of the metal complexes support its proposed structure and correspond well with the general formula $[M(L_2)X_2]$ where L = ligand; M = Co(II) Ni(II) and X = Cl^- , CH_3COO^- . The molar conductivity (Λ_m) of transition metal complexes measured in 1×10^{-3} mol L^{-1} DMSO at room temperature are too low to account for any dissociation, therefore the complexes are considered to be non-electrolytes (Table 2).

Schematic illustration of synthesis of the ligand (L) and its metal complexes is shown Scheme 1. Ligand (L) are prepared by [1+2] condensation reaction of phthalic acid and furfurylamine, further cyclized with different transition metals by mixing 2:1 ratio of the ligand with corresponding metal (Co, Ni) chloride and acetate salts. The obtained complexes are microcrystalline solids which are stable in air, are soluble in DMF, DMSO, sparingly soluble in MeOH, EtOH and DCM but insoluble in water.

3.1. FTIR Spectra

The emergence of new bands attributes for amide groups at 1648 $\nu(C=O)$ amide I, 1585 $\nu(C-N)$ amide II (Table 2) [37,38]. A sharp band observed in the region 3493 cm^{-1} could be allocated to $\nu(N-H)$ of the secondary amino group [39]. The amide $C=O$ stretch (I) of ligand is shifted to lower wave number by ca. 15-28 cm^{-1} , indicating that it participates as a coordinating site (Table 3). This coordination behavior shows how a ligand with multiple binding sites can coordinate to obtain a simple but stable geometry. The carbonyl groups which are more closer to the metal ion center maintaining less M-L bond distance, participate in the complexation, On complexation the position of $\nu(C=O)$ bands shifted to lower frequency compared to ligand, whereas the N-H band remains almost unaltered, which indicates that the coordination takes place through the oxygen $[O_4]$ group and a new band appears in the range 429-460 cm^{-1} which could be attributed to $\nu(M-O)$, also designates that the flow of electron density towards the metal atom is through the oxygen group [40]. Another medium intensity band in the region of 348 and 358 cm^{-1} has been assigned to $\nu(M-Cl)$ of LM_1 and LM_2 complexes. The presence of bands in the region 1595-1560 cm^{-1} and 1300-1315 cm^{-1} are characteristic of asymmetric and symmetric COO^- stretching vibrations respectively with $\Delta\nu = \sim 250$ cm^{-1} in complexes LM_3 and LM_4 .

Table 3. Relevant IR spectral peaks (cm^{-1}) and their assignments

Compound	ν N-H	Amide-I [$\nu C=O$]	Amide II [$\nu C-N$]	ν M-O	ν M-Cl	ν M-COO
L	3493	1648	1585			
LM_1	3156	1628	1554	455	358	...
LM_2	3155	1634	1574	429	348	...
LM_3	3170	1635	1562	460	...	1595-1560
LM_4	3152	1620	1565	452	...	1330-1315

3.2. ^1H NMR Spectra

Since aromatic protons of the ligand are in three different aromatic environments, it shows a multiplet in the region of 8.75-8.77 ppm Ar-CH (furfurylamine ring, O-C-H) (2H, m), 8.17-8.19 ppm Ar-CH (furfurylamine ring, O-C=C-H) (4H, m) and 7.41-7.43 ppm Ar-CH (Pthallic acid ring, C-H) (4H, m). A sharp singlet at 12.29 ppm which is associated to amide CO-NH, (2H) [41,42]. Due to paramagnetic effect of metal(II) ions, the above proton signals undergo down field shifting in all metal complexes and therefore sustenance the coordination of the ligand towards the metal ions [37,38]. The ^1H NMR spectral data for the ligand and its metal complexes is presented in Table 4.

Table 4. ^1H NMR data of ligand and its metal complexes.

Compound	^1H NMR assignment	δ (ppm)
Ligand (L)	(m; 2H; Ar-CH (Furfurylamine ring, O-C-H))	8.75-8.77
	(m; 4H; Ar-CH (Furfurylamine ring, O-C=C-H))	8.17-8.19
	(m; 4H; Ar-CH (Pthallic acid ring, C-H))	7.41-7.43
	(s; 2H; amide CO-NH)	12.29
LM ₁	(m; 2H; Ar-CH (Furfurylamine ring, O-C-H))	7.80-7.85
	(m; 4H; Ar-CH (Furfurylamine ring, O-C=C-H))	7.22-7.25
	(m; 4H; Ar-CH (Pthallic acid ring, C-H))	6.46-6.49
	(s; 2H; amide CO-NH)	11.85
LM ₂	(m; 2H; Ar-CH (Furfurylamine ring, O-C-H))	7.77-7.79
	(m; 4H; Ar-CH (Furfurylamine ring, O-C=C-H))	7.18-7.20
	(m; 4H; Ar-CH (Pthallic acid ring, C-H))	6.45-6.47
	(s; 2H; amide CO-NH)	11.95
LM ₃	(m; 2H; Ar-CH (Furfurylamine ring, O-C-H))	7.85-7.88
	(m; 4H; Ar-CH (Furfurylamine ring, O-C=C-H))	7.20-7.22
	(m; 4H; Ar-CH (Pthallic acid ring, C-H))	6.44-6.45
	(s; 2H; amide CO-NH)	11.90
LM ₄	(m; 2H; Ar-CH (Furfurylamine ring, O-C-H))	7.87-7.90
	(m; 4H; Ar-CH (Furfurylamine ring, O-C=C-H))	7.21-7.23
	(m; 4H; Ar-CH (Pthallic acid ring, C-H))	6.47-6.50
	(s; 2H; amide CO-NH)	11.92

3.3. Electro Spray Ionization Mass Spectra (ESI-MS)

The proposed formula of the ligand (L) is conformed by the mass spectra showing a peak at m/z 325 corresponding to the moiety $[(\text{C}_{18}\text{H}_{16}\text{N}_2\text{O}_4)^+]$ atomic mass m/z 324.34]. The series of peaks in the range m/z 96, 135.7, 185.6, 240, 342 etc, may be assigned to various fragments. Their intensity gives an idea of stability of fragments. Due to occurrence of isotopic chlorine in low quantities, $[\text{M}+2]^+$ bits were spotted in LM₁ & LM₂ metal complexes [43]. In several incidents, the molecular ion peak was also coupled with the solvent, water molecules and some adduct ions from the mobile phase solution [44].

3.4. Thermo Gravimetric Analysis (TG/DTA)

To conform the thermal stability of the synthesized compounds under investigation, thermal analysis (TG/DTA) of these compounds (LM_1 - LM_4) was carried out under nitrogen atmosphere at the heating rate of $10^\circ\text{C}/\text{min}$. The stability of the ligand was observed up to 150°C and shows a continuous weight loss up to 298°C , as a result, the entire ligand was decomposed in a single step. Two endothermic peaks were observed by DTA of the investigated ligand; one endothermic peak at 128°C and second endothermic peak at 295°C which corresponds to the melting and the first inflection point [45]. The thermogravimetric analysis was employed as a probe for the verification of the associated water or solvent molecules to be in coordination sphere or in crystalline form [46]. The TG profiles of metal complexes revealing that the synthesized metal complexes are more stable as compared to the free ligand and does not decompose below the temperatures of 300°C . It is very interesting to note that the complexes gain 5-7 % weight in the temperature range of 355 - 380°C and no further decomposition was observed. This weight gain of complexes may be accredited to the migration of the metal (M_{layer}) to the new vacant sites produced by the partial reduction of M^{4+} to M^{2+} in case of cobalt and nickel, then subsequent oxidation of M^{1+} , M^{2+} in cobalt and nickel complexes respectively [47,48].

3.5. Electronic spectra and magnetic studies

Cobalt (II) complexes (LM_1 and LM_3)

The electronic spectra of cobalt(II) complexes exhibit absorption in the region 11,240-11,420 ($\epsilon = 72$ - $74 \text{ L mol}^{-1}\text{cm}^{-1}$), 14,720-14,786 ($\epsilon = 81$ - $89 \text{ L mol}^{-1}\text{cm}^{-1}$), 18,650-18,695 ($\epsilon = 90$ - $95 \text{ L mol}^{-1}\text{cm}^{-1}$) and 32,710-33,365 ($\epsilon = 139$ - $141 \text{ L mol}^{-1}\text{cm}^{-1}$). These bands may be assigned to the transitions ${}^4T_{1g}(\text{F}) \rightarrow {}^4T_{2g}(\text{F})$ (ν_1), ${}^4T_{1g} \rightarrow {}^4A_{2g}$ (ν_2) and ${}^4T_{1g}(\text{F}) \rightarrow {}^4T_{2g}(\text{P})$ (ν_3) transitions respectively, and fourth band may be due to charge transfer between ligand to metal, signifying an octahedral geometry around Co(II) ion [49]. Magnetic moment of LM_1 and LM_3 recline in the range of 4.86–4.92 B.M corresponding to three unpaired electrons at room temperature. Orbital angular momentum and total spin angular momentum relay on the value of magnetic moment [50].

Nickel (II) complexes (LM_2 and LM_4)

The electronic spectra of Ni(II) complexes exhibit three absorption bands in the range 10,186-10,198 ($\epsilon = 52$ - $53 \text{ L mol}^{-1}\text{cm}^{-1}$), 18,635-18,657 ($\epsilon = 85$ - $92 \text{ L mol}^{-1}\text{cm}^{-1}$) and 20,380-21,480 ($\epsilon = 142$ - $155 \text{ L mol}^{-1}\text{cm}^{-1}$). These bands may be assigned to ${}^3A_{2g}(\text{F}) \rightarrow {}^3T_{2g}(\text{F})$ (ν_1), ${}^3A_{2g}(\text{F}) \rightarrow {}^3T_{1g}(\text{F})$ (ν_2), and ${}^3A_{2g}(\text{F}) \rightarrow {}^3T_{1g}(\text{P})$ (ν_3), respectively [51]. the magnetic moment of LM_2 and LM_4 at room temperature lie in the range of 2.72-2.89 B.M corresponding to two unpaired electrons (Table. 3). Thus, on the basis of spectral studies complexes were assigned to have a six coordinated distorted octahedral geometry as shown in Scheme 1. The absorption bands for the electronic spectra of metal acetates along with their magnetic moments were give in (Table. 5)

Table 5. Magnetic moment and electronic spectral data of metal complexes

Compounds	Spectral bands λ_{\max} (cm ⁻¹)	ϵ_{\max} (L mol ⁻¹ cm ⁻¹)	μ_{eff} (B.M) ^a
LM ₁	11240, 14720, 18650, 32710	72, 81, 90, 139	4.86
LM ₂	10186, 18635, 20380	52, 85, 142	2.78
LM ₃	12320, 16110, 19330, 29310	70, 78, 89, 135	4.91
LM ₄	14110, 18640, 24450	75, 80, 133	2.88

3.6 Solid state electrical conductivity

The solid state electrical conductivity measurements were performed under vacuum (103 mmhg) and the samples were inserted in to the electrical furnace. Before recording the electric conductivity, the system was allowed to stabilize for 30 min. The rate of temperature change with time was kept to a minimum (2 °C/min) by means of copper constantan thermocouple. In case of semiconducting materials several parameters like thermal excitation, impurities, lattice defects, degree of crystallinity and temperature affect the conduction mechanism. The temperature dependence of the solid state conductivity (σ) of the synthesized compounds in pressed pellet form have been measured in the temperature range 308-438 K using two probe method and obbying the following equation:

$$\sigma = \sigma_0 \exp^{-\Delta E/KT}$$

where σ_0 is a constant for the conductivity independent of temperature, ΔE is the activation energy of the conduction process, K is the Boltzmann's constant and T is the absolute temperature. Fig. 4 shows the plots of log conductivity vs. $1000/T$ for all synthesized compounds and have been found to be linear over a studied temperature range indicating the semiconducting behaviour of the complexes i.e. with increasing temperature there is an increase in electrical conductivity and decrease upon cooling over the studied temperature range [52]. The semiconducting behavior of the synthesized complexes may be also due to the presence of various π - π interactions. The electrical conductivity increased on increase in temperature as in case of semiconductors. The conductivity curves for all the synthesized metal complexes showed a semiconducting behavior in the range 308-438 K. The electrical conductivity of Co complexes is higher than Ni complexes at room temperature and the activation energy of electrical conduction lies in the range 0.35-0.52 eV. Repeated measurements showed a similar conductivity pattern for all the complexes confirming the temperature dependence of the conductivity of the complexes. The counter cation played an important role to facilitate conduction mechanism and transferring the electrons more easily from valance band to the conduction band, suggesting that the conduction occurred through hopping mechanism.

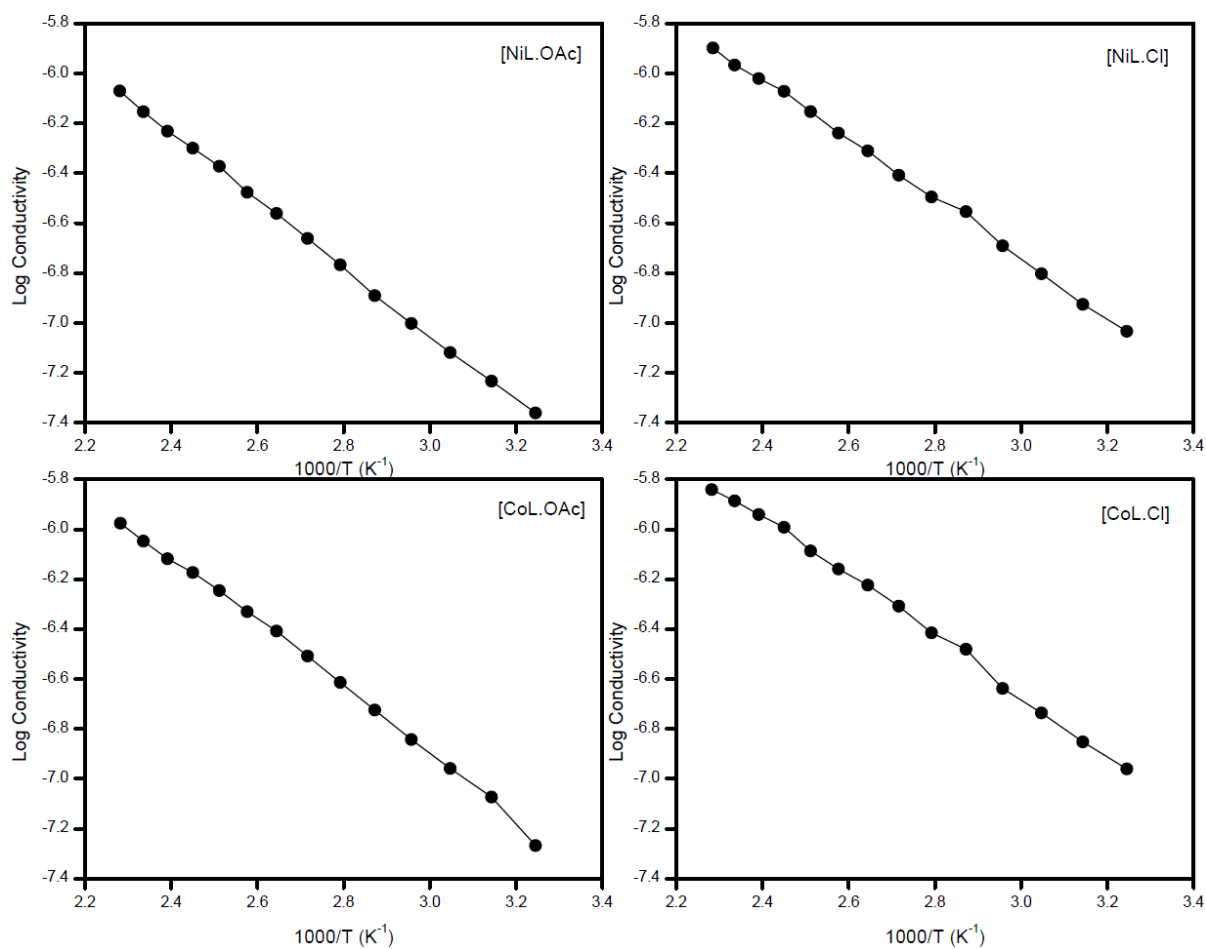


Figure 4. The electrical conductivity of Ni(II) and Co(II) complexes

3.7. Molecular modelling

The single crystals for ligand and its Ni(II) and Co(II) metal complexes could not be obtained, therefore it was a valuable consideration to acquire structural information of these synthesized compounds by molecular modelling. Geometry optimization was carried out by using CHEM 3D Ultra software for ligand (L) and $[\text{Co}(\text{L}_2)\text{Cl}_2]$. Several successful cycles of energy minimization were performed for each of the molecules. The theoretical physical parameters such as bond lengths and bond angles were calculated as per the 3D structure of the synthesised compounds and the representative data is presented in Tables 6-11. The atoms in the 3D structure of the synthesized compounds are represented by the symbol of the atom for the ease of looking over the bond lengths and bond angles between the atoms. The data presented in Tables 6-11 are calculated values acquired after the energy optimization in CHEM 3D Ultra graphic software, though the values of optimal bond length and optimal bond angle are the most standard (desirable/favorable) bond lengths and bond angles ascertained by the builder unit of the CHEM 3D graphic software. Because of the limitations of the software, some of the values of standard bond lengths and bond angles are missing, as this was previously noticed in modelling of other systems [53,54]. In most of the cases, the actual bond lengths

and bond angles are close to the optimal values, and thus the proposed structures of the synthesized compounds (Fig. 1-3) as well as of the others are acceptable [53,54].

Table 6. Various bond lengths (Å) of Ligand (L)

Sr. No	Atoms	Actual bond lengths	Optimal bond lengths	Sr. No	Atoms	Actual bond lengths	Optimal bond lengths
1	N(24)-H(40)	1.012	1.022	22	C(8)-C(9)	1.395	1.42
2	C(23)-H(39)	1.113	1.113	23	C(19)-O(18)	1.358	1.323
3	C(23)-H(38)	1.113	1.113	24	C(21)-O(18)	1.358	1.323
4	C(22)-H(37)	1.1	1.1	25	C(22)-C(21)	1.375	1.42
5	C(20)-H(36)	1.1	1.1	26	C(20)-C(22)	1.416	1.42
6	C(19)-H(35)	1.1	1.1	27	C(19)-C(20)	1.376	1.42
7	C(11)-H(34)	1.1	1.1	28	C(2)-O(1)	1.358	1.323
8	C(10)-H(33)	1.1	1.1	29	C(4)-O(1)	1.358	1.323
9	C(9)-H(32)	1.1	1.1	30	C(5)-C(4)	1.375	1.42
10	C(8)-H(31)	1.1	1.1	31	C(3)-C(5)	1.416	1.42
11	N(7)-H(30)	1.012	1.022	32	C(2)-C(3)	1.376	1.42
12	C(6)-H(29)	1.113	1.113	33	C(14)-N(24)	1.369	1.369
13	C(6)-H(28)	1.113	1.113	34	C(23)-N(24)	1.45	1.46
14	C(5)-H(27)	1.1	1.1	35	C(21)-C(23)	1.497	1.497
15	C(3)-H(26)	1.1	1.1	36	N(7)-C(15)	1.369	1.369
16	C(2)-H(25)	1.1	1.1	37	C(14)-O(17)	1.208	1.208
17	C(8)-C(10)	1.395	1.42	38	C(15)-O(16)	1.208	1.208
18	C(12)-C(10)	1.395	1.42	39	C(13)-C(15)	1.351	1.517
19	C(13)-C(12)	1.395	1.42	40	C(12)-C(14)	1.351	1.517
20	C(11)-C(13)	1.395	1.42	41	C(6)-N(7)	1.45	1.46
21	C(9)-C(11)	1.395	1.42	42	C(4)-C(6)	1.497	1.497

Table 7. Various bond angles (°) of Ligand(L)

Sr. No	Atoms	Actual bond angles	Optimal bond angles	Sr. No	Atoms	Actual bond angles	Optimal bond angles
1.	C(4)-O(1)-C(2)	106.819	113.95	35.	C(8)-C(9)-C(11)	119.997	
2.	H(36)-C(20)-C(19)	126.929	120	36.	C(14)-C(12)-C(10)	120.001	117.6
3.	H(36)-C(20)-C(22)	126.929	120	37.	C(14)-C(12)-C(13)	120.001	117.6
4.	C(19)-C(20)-C(22)	106.142		38.	C(10)-C(12)-C(13)	119.997	120
5.	H(35)-C(19)-C(20)	124.777	120	39.	H(34)-C(11)-C(9)	120	120
6.	H(35)-C(19)-O(18)	124.776	108	40.	H(34)-C(11)-C(13)	120	120
7.	C(20)-C(19)-O(18)	110.447	118.1	41.	C(9)-C(11)-C(13)	120	
8.	H(37)-C(22)-C(20)	126.924	120	42.	C(12)-C(13)-C(11)	120.003	120
9.	H(37)-C(22)-C(21)	126.923	120	43.	C(12)-C(13)-C(15)	119.999	117.6
10.	C(20)-C(22)-C(21)	106.153		44.	C(11)-C(13)-C(15)	119.999	117.6
11.	C(19)-O(18)-C(21)	106.819	113.95	45.	O(16)-C(15)-C(13)	120	123
12.	C(22)-C(21)-O(18)	110.439	120	46.	O(16)-C(15)-N(7)	120	122.6
13.	C(22)-C(21)-C(23)	124.78	121.4	47.	C(13)-C(15)-N(7)	120	112.74
14.	O(18)-C(21)-C(23)	124.781	120	48.	H(30)-N(7)-C(15)	120	117.4
15.	H(39)-C(23)-H(38)	109.52	109.4	49.	H(30)-N(7)-C(6)	120	118
16.	H(39)-C(23)-C(21)	109.462	109.41	50.	C(15)-N(7)-C(6)	120	
17.	H(39)-C(23)-N(24)	109.462		51.	H(29)-C(6)-H(28)	109.52	109.4
18.	H(38)-C(23)-C(21)	109.442	109.41	52.	H(29)-C(6)-N(7)	109.461	
19.	H(38)-C(23)-N(24)	109.442		53.	H(29)-C(6)-C(4)	109.462	109.41
20.	C(21)-C(23)-N(24)	109.5		54.	H(28)-C(6)-N(7)	109.442	
21.	H(40)-N(24)-C(23)	120	118	55.	H(28)-C(6)-C(4)	109.442	109.41
22.	H(40)-N(24)-C(14)	120	117.4	56.	N(7)-C(6)-C(4)	109.5	
23.	C(23)-N(24)-C(14)	120		57.	H(27)-C(5)-C(3)	126.923	120
24.	O(17)-C(14)-N(24)	120	122.6	58.	H(27)-C(5)-C(4)	126.924	120
25.	O(17)-C(14)-C(12)	120	123	59.	C(3)-C(5)-C(4)	106.153	
26.	N(24)-C(14)-C(12)	120	112.74	60.	O(1)-C(4)-C(6)	124.781	120
27.	H(33)-C(10)-C(12)	120	120	61.	O(1)-C(4)-C(5)	110.439	120
28.	H(33)-C(10)-C(8)	120	120	62.	C(6)-C(4)-C(5)	124.78	121.4

29.	C(12)-C(10)-C(8)	120		63.	H(26)-C(3)-C(5)	126.929	120
30.	H(31)-C(8)-C(10)	119.999	120	64.	H(26)-C(3)-C(2)	126.929	120
31.	H(31)-C(8)-C(9)	119.998	120	65.	C(5)-C(3)-C(2)	106.142	
32.	C(10)-C(8)-C(9)	120.003		66.	O(1)-C(2)-H(25)	124.777	108
33.	H(32)-C(9)-C(8)	120.002	120	67.	O(1)-C(2)-C(3)	110.447	118.1
34.	H(32)-C(9)-C(11)	120.002	120	68.	H(25)-C(2)-C(3)	124.777	120

Table 8. Various bond lengths (Å) of [CoL₂Cl₂] metal complex

Sr. No	Atoms	Actual bond lengths	Optimal bond lengths	Sr. No	Atoms	Actual bond lengths	Optimal bond lengths
1.	N(48)-H(83)	1.022	1.022	46.	C(20)-C(22)	1.508	1.42
2.	C(47)-H(82)	1.113	1.113	47.	C(19)-C(20)	1.589	1.42
3.	C(47)-H(81)	1.113	1.113	48.	C(2)-O(1)	1.787	1.323
4.	C(46)-H(80)	1.1	1.1	49.	C(4)-O(1)	1.315	1.323
5.	C(44)-H(79)	1.1	1.1	50.	C(5)-C(4)	1.7	1.42
6.	C(43)-H(78)	1.1	1.1	51.	C(3)-C(5)	1.386	1.42
7.	C(35)-H(77)	1.004	1.1	52.	C(2)-C(3)	1.676	1.42
8.	C(34)-H(76)	1.1	1.1	53.	Co(49)-Cl(51)	2.363	
9.	C(33)-H(75)	1.1	1.1	54.	Co(49)-Cl(50)	2.814	
10.	C(32)-H(74)	1.1	1.1	55.	O(17)-Co(49)	1.962	0.6
11.	N(31)-H(73)	1.022	1.022	56.	O(16)-Co(49)	1.583	0.6
12.	C(30)-H(72)	1.113	1.113	57.	O(41)-Co(49)	1.253	0.6
13.	C(30)-H(71)	1.107	1.113	58.	O(40)-Co(49)	1.393	0.6
14.	C(29)-H(70)	1.1	1.1	59.	C(38)-N(48)	1.611	1.369
15.	C(27)-H(69)	1.1	1.1	60.	C(47)-N(48)	1.466	1.46
16.	C(26)-H(68)	1.1	1.1	61.	C(45)-C(47)	1.755	1.497
17.	N(24)-H(67)	1.022	1.022	62.	N(31)-C(39)	1.805	1.369
18.	C(23)-H(66)	1.113	1.113	63.	C(38)-O(41)	1.415	1.208
19.	C(23)-H(65)	1.113	1.113	64.	C(39)-O(40)	1.259	1.208
20.	C(22)-H(64)	1.1	1.1	65.	C(37)-C(39)	1.588	1.517
21.	C(20)-H(63)	1.1	1.1	66.	C(36)-C(38)	1.391	1.517
22.	C(19)-H(62)	1.1	1.1	67.	C(37)-C(36)	1.42	1.42
23.	C(11)-H(61)	1.144	1.1	68.	C(37)-C(35)	1.269	1.42
24.	C(10)-H(60)	1.117	1.1	69.	C(36)-C(34)	1.593	1.42
25.	C(9)-H(59)	1.101	1.1	70.	C(35)-C(33)	1.671	1.42
26.	C(8)-H(58)	1.1	1.1	71.	C(34)-C(32)	1.325	1.42
27.	N(7)-H(57)	1.022	1.022	72.	C(33)-C(32)	1.355	1.42
28.	C(6)-H(56)	1.113	1.113	73.	C(30)-N(31)	1.454	1.46
29.	C(6)-H(55)	1.113	1.113	74.	C(28)-C(30)	1.265	1.497
30.	C(5)-H(54)	1.1	1.1	75.	C(14)-N(24)	1.591	1.369
31.	C(3)-H(53)	1.1	1.1	76.	C(23)-N(24)	1.611	1.46
32.	C(2)-H(52)	1.1	1.1	77.	C(21)-C(23)	1.435	1.497
33.	C(43)-O(42)	1.574	1.323	78.	N(7)-C(15)	1.567	1.369
34.	C(45)-O(42)	1.72	1.323	79.	C(14)-O(17)	1.285	1.208
35.	C(46)-C(45)	1.427	1.42	80.	C(15)-O(16)	1.181	1.208
36.	C(44)-C(46)	1.844	1.42	81.	C(13)-C(15)	1.621	1.517
37.	C(43)-C(44)	1.711	1.42	82.	C(12)-C(14)	1.607	1.517
38.	C(26)-O(25)	1.74	1.323	83.	C(13)-C(12)	1.47	1.42
39.	C(28)-O(25)	1.794	1.323	84.	C(13)-C(11)	1.421	1.42
40.	C(29)-C(28)	1.897	1.42	85.	C(12)-C(10)	1.49	1.42
41.	C(27)-C(29)	1.331	1.42	86.	C(11)-C(9)	1.46	1.42
42.	C(26)-C(27)	1.802	1.42	87.	C(10)-C(8)	1.436	1.42
43.	C(19)-O(18)	1.296	1.323	88.	C(9)-C(8)	1.421	1.42

44.	C(21)-O(18)	1.898	1.323	89.	C(6)-N(7)	1.319	1.46
45.	C(22)-C(21)	1.506	1.42	90.	C(4)-C(6)	1.736	1.497

Table 9. Various bond angles ($^{\circ}$) of [CoL₂Cl₂] metal complex.

Sr. No	Atoms	Actual bond angles	Optimal bond angles	Sr. No	Atoms	Actual bond angles	Optimal bond angles
1.	H(79)-C(44)-C(46)	124.646	120	51.	C(22)-C(21)-C(23)	127.544	121.4
2.	H(79)-C(44)-C(43)	124.645	120	52.	H(66)-C(23)-H(65)	113.921	109.4
3.	C(46)-C(44)-C(43)	110.706		53.	H(66)-C(23)-N(24)	109.5	
4.	H(78)-C(43)-O(42)	127.261	108	54.	H(66)-C(23)-C(21)	109.41	109.41
5.	H(78)-C(43)-C(44)	139.261	120	55.	H(65)-C(23)-N(24)	109.5	
6.	O(42)-C(43)-C(44)	93.473	118.1	56.	H(65)-C(23)-C(21)	109.41	109.41
7.	H(80)-C(46)-C(45)	125.841	120	57.	N(24)-C(23)-C(21)	104.692	
8.	H(80)-C(46)-C(44)	125.841	120	58.	H(83)-N(48)-C(38)	126.381	117.4
9.	C(45)-C(46)-C(44)	108.315		59.	H(83)-N(48)-C(47)	126.981	118
10.	C(43)-O(42)-C(45)	124.283	113.95	60.	C(38)-N(48)-C(47)	106.634	
11.	O(42)-C(45)-C(46)	102.863	120	61.	H(73)-N(31)-C(39)	141.405	117.4
12.	O(42)-C(45)-C(47)	141.937	120	62.	H(73)-N(31)-C(30)	142.005	118
13.	C(46)-C(45)-C(47)	114.805	121.4	63.	C(39)-N(31)-C(30)	76.583	
14.	H(82)-C(47)-H(81)	116.744	109.4	64.	H(67)-N(24)-C(14)	122.554	117.4
15.	H(82)-C(47)-N(48)	109.5		65.	H(67)-N(24)-C(23)	123.154	118
16.	H(82)-C(47)-C(45)	109.41	109.41	66.	C(14)-N(24)-C(23)	114.289	
17.	H(81)-C(47)-N(48)	109.5		67.	H(75)-C(33)-C(35)	119.995	120
18.	H(81)-C(47)-C(45)	109.41	109.41	68.	H(75)-C(33)-C(32)	119.995	120
19.	N(48)-C(47)-C(45)	101.14		69.	C(35)-C(33)-C(32)	120.008	
20.	H(69)-C(27)-C(29)	123.275	120	70.	H(74)-C(32)-C(34)	119.675	120
21.	H(69)-C(27)-C(26)	123.275	120	71.	H(74)-C(32)-C(33)	119.676	120
22.	C(29)-C(27)-C(26)	113.446		72.	C(34)-C(32)-C(33)	120.647	
23.	H(68)-C(26)-O(25)	122.245	108	73.	N(31)-C(39)-O(40)	137.085	122.6
24.	H(68)-C(26)-C(27)	134.245	120	74.	N(31)-C(39)-C(37)	101.301	112.74
25.	O(25)-C(26)-C(27)	103.506	118.1	75.	O(40)-C(39)-C(37)	112.739	123
26.	H(70)-C(29)-C(28)	122.166	120	76.	H(77)-C(35)-C(37)	119.851	120
27.	H(70)-C(29)-C(27)	122.167	120	77.	H(77)-C(35)-C(33)	119.851	120
28.	C(28)-C(29)-C(27)	115.664		78.	C(37)-C(35)-C(33)	120.296	
29.	C(26)-O(25)-C(28)	108.88	113.95	79.	H(76)-C(34)-C(36)	121.791	120
30.	O(25)-C(28)-C(29)	97.935	120	80.	H(76)-C(34)-C(32)	121.791	120
31.	O(25)-C(28)-C(30)	125.293	120	81.	C(36)-C(34)-C(32)	116.416	
32.	C(29)-C(28)-C(30)	136.135	121.4	82.	C(39)-C(37)-C(36)	121.398	117.6
33.	H(72)-C(30)-H(71)	124.057	109.4	83.	C(39)-C(37)-C(35)	121.907	117.6
34.	H(72)-C(30)-N(31)	109.5		84.	C(36)-C(37)-C(35)	116.523	120
35.	H(72)-C(30)-C(28)	109.41	109.41	85.	C(38)-C(36)-C(37)	115.386	117.6
36.	H(71)-C(30)-N(31)	109.501		86.	C(38)-C(36)-C(34)	113.587	117.6
37.	H(71)-C(30)-C(28)	109.41	109.41	87.	C(37)-C(36)-C(34)	124.389	120
38.	N(31)-C(30)-C(28)	89.51		88.	N(48)-C(38)-O(41)	132.386	122.6
39.	H(63)-C(20)-C(22)	123.772	120	89.	N(48)-C(38)-C(36)	119.183	112.74
40.	H(63)-C(20)-C(19)	123.773	120	90.	O(41)-C(38)-C(36)	104.506	123
41.	C(22)-C(20)-C(19)	112.452		91.	Co(49)-O(41)-C(38)	170	
42.	H(62)-C(19)-O(18)	115.518	108	92.	Co(49)-O(40)-C(39)	143.919	
43.	H(62)-C(19)-C(20)	127.517	120	93.	Co(49)-O(17)-C(14)	141.058	
44.	O(18)-C(19)-C(20)	116.962	118.1	94.	Cl(51)-Co(49)-Cl(50)	79.117	
45.	H(64)-C(22)-C(21)	129.545	120	95.	Cl(51)-Co(49)-O(17)	56.184	

46.	H(64)-C(22)-C(20)	129.544	120	96.	Cl(51)-Co(49)-O(16)	97.627	
47.	C(21)-C(22)-C(20)	100.907		97.	Cl(51)-Co(49)-O(41)	94.287	
48.	C(19)-O(18)-C(21)	95.603	113.95	98.	Cl(51)-Co(49)-O(40)	104.526	
49.	O(18)-C(21)-C(22)	109.169	120	99.	Cl(50)-Co(49)-O(17)	100.73	
50.	O(18)-C(21)-C(23)	118.743	120	100.	Cl(50)-Co(49)-O(16)	74.553	
01.	Cl(50)-Co(49)-O(41)	134.09		29.	C(15)-C(13)-C(11)	135.66	117.6
02.	Cl(50)-Co(49)-O(40)	66.798		30.	C(12)-C(13)-C(11)	122.104	120
03.	O(17)-Co(49)-O(16)	55.106		31.	N(7)-C(15)-O(16)	120.567	122.6
04.	O(17)-Co(49)-O(41)	113.039		32.	N(7)-C(15)-C(13)	88.605	112.74
05.	O(17)-Co(49)-O(40)	159.765		33.	O(16)-C(15)-C(13)	150.73	123
06.	O(16)-Co(49)-O(41)	150.823		34.	H(57)-N(7)-C(15)	129.363	117.4
07.	O(16)-Co(49)-O(40)	130.104		35.	H(57)-N(7)-C(6)	129.963	118
08.	O(41)-Co(49)-O(40)	71.299		36.	C(15)-N(7)-C(6)	100.669	
09.	Co(49)-O(16)-C(15)	151.687		37.	H(56)-C(6)-H(55)	106.421	109.4
10.	H(59)-C(9)-C(11)	122.268	120	38.	H(56)-C(6)-N(7)	109.5	
11.	H(59)-C(9)-C(8)	119.241	120	39.	H(56)-C(6)-C(4)	109.41	109.41
12.	C(11)-C(9)-C(8)	118.472		40.	H(55)-C(6)-N(7)	109.499	
13.	H(58)-C(8)-C(10)	119.827	120	41.	H(55)-C(6)-C(4)	109.41	109.41
14.	H(58)-C(8)-C(9)	118.979	120	42.	N(7)-C(6)-C(4)	112.42	
15.	C(10)-C(8)-C(9)	121.172		43.	H(54)-C(5)-C(4)	124.998	120
16.	N(24)-C(14)-O(17)	122.401	122.6	44.	H(54)-C(5)-C(3)	124.999	120
17.	N(24)-C(14)-C(12)	79.884	112.74	45.	C(4)-C(5)-C(3)	110	
18.	O(17)-C(14)-C(12)	155.178	123	46.	O(1)-C(4)-C(5)	124.983	120
19.	H(60)-C(10)-C(12)	121.314	120	47.	O(1)-C(4)-C(6)	118.388	120
20.	H(60)-C(10)-C(8)	116.771	120	48.	C(5)-C(4)-C(6)	116.587	121.4
21.	C(12)-C(10)-C(8)	121.885		49.	H(53)-C(3)-C(5)	131.149	120
22.	H(61)-C(11)-C(13)	123.457	120	50.	H(53)-C(3)-C(2)	131.15	120
23.	H(61)-C(11)-C(9)	115.386	120	51.	C(5)-C(3)-C(2)	97.697	
24.	C(13)-C(11)-C(9)	121.128		52.	H(52)-C(2)-O(1)	115.701	108
25.	C(14)-C(12)-C(13)	98.066	117.6	53.	H(52)-C(2)-C(3)	127.7	120
26.	C(14)-C(12)-C(10)	146.745	117.6	54.	O(1)-C(2)-C(3)	116.596	118.1
27.	C(13)-C(12)-C(10)	115.008	120	55.	C(2)-O(1)-C(4)	88.608	113.95
28.	C(15)-C(13)-C(12)	102.154	117.6				

Table 10. Various bond lengths (Å) of [NiL₂Cl₂] metal complex

Sr. No	Atoms	Actual bond lengths	Optimal bond lengths	Sr. No	Atoms	Actual bond lengths	Optimal bond lengths
1.	N(48)-H(83)	1.024	1.022	46.	C(20)-C(22)	1.34	1.42
2.	C(47)-H(82)	1.118	1.113	47.	C(19)-C(20)	1.338	1.42
3.	C(47)-H(81)	1.115	1.113	48.	C(2)-O(1)	1.229	1.323
4.	C(46)-H(80)	1.107	1.1	49.	C(4)-O(1)	1.232	1.323
5.	C(44)-H(79)	1.094	1.1	50.	C(5)-C(4)	1.34	1.42
6.	C(43)-H(78)	1.097	1.1	51.	C(3)-C(5)	1.338	1.42
7.	C(35)-H(77)	1.067	1.1	52.	C(2)-C(3)	1.338	1.42
8.	C(34)-H(76)	1.084	1.1	53.	Ni(49)-Cl(51)	2.354	
9.	C(33)-H(75)	1.104	1.1	54.	Ni(49)-Cl(50)	1.94	
10.	C(32)-H(74)	1.096	1.1	55.	O(16)-Ni(49)	1.824	
11.	N(31)-H(73)	1.012	1.022	56.	O(17)-Ni(49)	1.838	
12.	C(30)-H(72)	1.112	1.113	57.	O(40)-Ni(49)	1.846	
13.	C(30)-H(71)	1.103	1.113	58.	O(41)-Ni(49)	1.86	

14.	C(29)-H(70)	1.092	1.1	59.	C(38)-N(48)	1.395	1.369
15.	C(27)-H(69)	1.097	1.1	60.	C(47)-N(48)	1.473	1.46
16.	C(26)-H(68)	1.098	1.1	61.	C(45)-C(47)	1.574	1.497
17.	N(24)-H(67)	1.018	1.022	62.	N(31)-C(39)	1.358	1.369
18.	C(23)-H(66)	1.118	1.113	63.	C(38)-O(41)	1.234	1.208
19.	C(23)-H(65)	1.114	1.113	64.	C(39)-O(40)	1.228	1.208
20.	C(22)-H(64)	1.098	1.1	65.	C(37)-C(39)	1.376	1.517
21.	C(20)-H(63)	1.097	1.1	66.	C(36)-C(38)	1.34	1.517
22.	C(19)-H(62)	1.097	1.1	67.	C(37)-C(36)	1.369	1.42
23.	C(11)-H(61)	1.105	1.1	68.	C(37)-C(35)	1.345	1.42
24.	C(10)-H(60)	1.11	1.1	69.	C(36)-C(34)	1.364	1.42
25.	C(9)-H(59)	1.098	1.1	70.	C(35)-C(33)	1.337	1.42
26.	C(8)-H(58)	1.107	1.1	71.	C(34)-C(32)	1.33	1.42
27.	N(7)-H(57)	1.012	1.022	72.	C(33)-C(32)	1.331	1.42
28.	C(6)-H(56)	1.113	1.113	73.	C(30)-N(31)	1.451	1.46
29.	C(6)-H(55)	1.116	1.113	74.	C(28)-C(30)	1.513	1.497
30.	C(5)-H(54)	1.095	1.1	75.	C(14)-N(24)	1.377	1.369
31.	C(3)-H(53)	1.095	1.1	76.	C(23)-N(24)	1.478	1.46
32.	C(2)-H(52)	1.095	1.1	77.	C(21)-C(23)	1.515	1.497
33.	C(43)-O(42)	1.231	1.323	78.	N(7)-C(15)	1.381	1.369
34.	C(45)-O(42)	1.294	1.323	79.	C(14)-O(17)	1.206	1.208
35.	C(46)-C(45)	1.353	1.42	80.	C(15)-O(16)	1.226	1.208
36.	C(44)-C(46)	1.327	1.42	81.	C(13)-C(15)	1.369	1.517
37.	C(43)-C(44)	1.313	1.42	82.	C(12)-C(14)	1.345	1.517
38.	C(26)-O(25)	1.233	1.323	83.	C(13)-C(12)	1.352	1.42
39.	C(28)-O(25)	1.235	1.323	84.	C(13)-C(11)	1.352	1.42
40.	C(29)-C(28)	1.342	1.42	85.	C(12)-C(10)	1.35	1.42
41.	C(27)-C(29)	1.337	1.42	86.	C(11)-C(9)	1.339	1.42
42.	C(26)-C(27)	1.338	1.42	87.	C(10)-C(8)	1.339	1.42
43.	C(19)-O(18)	1.231	1.323	88.	C(9)-C(8)	1.336	1.42
44.	C(21)-O(18)	1.233	1.323	89.	C(6)-N(7)	1.467	1.46
45.	C(22)-C(21)	1.345	1.42	90.	C(4)-C(6)	1.5	1.497

Table 11. Various bond angles ($^{\circ}$) of $[\text{NiL}_2\text{Cl}_2]$ metal complex.

Sr. No	Atoms	Actual bond angles	Optimal bond angles	Sr. No	Atoms	Actual bond angles	Optimal bond angles
1.	H(79)-C(44)-C(46)	133.351	120	51.	C(22)-C(21)-C(23)	125.477	121.4
2.	H(79)-C(44)-C(43)	134.019	120	52.	H(66)-C(23)-H(65)	109.166	109.4
3.	C(46)-C(44)-C(43)	92.629		53.	H(66)-C(23)-N(24)	113.908	
4.	H(78)-C(43)-O(42)	119.314	108	54.	H(66)-C(23)-C(21)	105.228	109.41
5.	H(78)-C(43)-C(44)	130.228	120	55.	H(65)-C(23)-N(24)	109.369	
6.	O(42)-C(43)-C(44)	110.442	118.1	56.	H(65)-C(23)-C(21)	108.174	109.41
7.	H(80)-C(46)-C(45)	115.715	120	57.	N(24)-C(23)-C(21)	110.791	
8.	H(80)-C(46)-C(44)	116.922	120	58.	H(73)-N(31)-C(39)	111.56	117.4
9.	C(45)-C(46)-C(44)	127.351		59.	H(73)-N(31)-C(30)	114.36	118
10.	C(43)-O(42)-C(45)	123.151	113.95	60.	C(39)-N(31)-C(30)	132.292	
11.	O(42)-C(45)-C(46)	86.394	120	61.	N(31)-C(39)-O(40)	108.654	122.6
12.	O(42)-C(45)-C(47)	82.271	120	62.	N(31)-C(39)-C(37)	129.091	112.74
13.	C(46)-C(45)-C(47)	168.665	121.4	63.	O(40)-C(39)-C(37)	121.327	123

14.	H(82)-C(47)-H(81)	111.303	109.4	64.	H(77)-C(35)-C(37)	121.989	120
15.	H(82)-C(47)-N(48)	107.409		65.	H(77)-C(35)-C(33)	113.617	120
16.	H(82)-C(47)-C(45)	96.448	109.41	66.	C(37)-C(35)-C(33)	124.28	
17.	H(81)-C(47)-N(48)	108.68		67.	H(75)-C(33)-C(35)	121.585	120
18.	H(81)-C(47)-C(45)	110.29	109.41	68.	H(75)-C(33)-C(32)	117.648	120
19.	N(48)-C(47)-C(45)	121.942		69.	C(35)-C(33)-C(32)	120.58	
20.	H(69)-C(27)-C(29)	127.951	120	70.	H(74)-C(32)-C(34)	120.126	120
21.	H(69)-C(27)-C(26)	128.957	120	71.	H(74)-C(32)-C(33)	121.831	120
22.	C(29)-C(27)-C(26)	103.073		72.	C(34)-C(32)-C(33)	118.031	
23.	H(68)-C(26)-O(25)	117.774	108	73.	C(39)-C(37)-C(36)	121.971	117.6
24.	H(68)-C(26)-C(27)	129.896	120	74.	C(39)-C(37)-C(35)	124.116	117.6
25.	O(25)-C(26)-C(27)	112.316	118.1	75.	C(36)-C(37)-C(35)	113.911	120
26.	H(70)-C(29)-C(28)	127.059	120	76.	H(76)-C(34)-C(36)	123.308	120
27.	H(70)-C(29)-C(27)	127.11	120	77.	H(76)-C(34)-C(32)	115.534	120
28.	C(28)-C(29)-C(27)	105.78		78.	C(36)-C(34)-C(32)	121.072	
29.	C(26)-O(25)-C(28)	108.607	113.95	79.	H(83)-N(48)-C(38)	114.231	117.4
30.	O(25)-C(28)-C(29)	110.224	120	80.	H(83)-N(48)-C(47)	112.194	118
31.	O(25)-C(28)-C(30)	126.617	120	81.	C(38)-N(48)-C(47)	133.463	
32.	C(29)-C(28)-C(30)	122.623	121.4	82.	C(38)-C(36)-C(37)	120.544	117.6
33.	H(72)-C(30)-H(71)	109.518	109.4	83.	C(38)-C(36)-C(34)	117.543	117.6
34.	H(72)-C(30)-N(31)	106.483		84.	C(37)-C(36)-C(34)	121.704	120
35.	H(72)-C(30)-C(28)	109.289	109.41	85.	N(48)-C(38)-O(41)	133.194	122.6
36.	H(71)-C(30)-N(31)	120.161		86.	N(48)-C(38)-C(36)	109.987	112.74
37.	H(71)-C(30)-C(28)	108.855	109.41	87.	O(41)-C(38)-C(36)	111.999	123
38.	N(31)-C(30)-C(28)	102.006		88.	Ni(49)-O(41)-C(38)	110.698	
39.	H(63)-C(20)-C(22)	128.309	120	89.	Ni(49)-O(40)-C(39)	110.828	
40.	H(63)-C(20)-C(19)	128.101	120	90.	H(67)-N(24)-C(14)	117.932	117.4
41.	C(22)-C(20)-C(19)	103.589		91.	H(67)-N(24)-C(23)	116.702	118
42.	H(62)-C(19)-O(18)	117.539	108	92.	C(14)-N(24)-C(23)	125.068	
43.	H(62)-C(19)-C(20)	130.555	120	93.	Ni(49)-O(17)-C(14)	111.516	
44.	O(18)-C(19)-C(20)	111.906	118.1	94.	N(24)-C(14)-O(17)	120.274	122.6
45.	H(64)-C(22)-C(21)	127.675	120	95.	N(24)-C(14)-C(12)	118.718	112.74
46.	H(64)-C(22)-C(20)	127.161	120	96.	O(17)-C(14)-C(12)	112.683	123
47.	C(21)-C(22)-C(20)	105.162		97.	H(60)-C(10)-C(12)	123.873	120
48.	C(19)-O(18)-C(21)	108.97	113.95	98.	H(60)-C(10)-C(8)	114.034	120
49.	O(18)-C(21)-C(22)	110.372	120	99.	C(12)-C(10)-C(8)	121.988	
50.	O(18)-C(21)-C(23)	124.143	120	100.	H(58)-C(8)-C(10)	122.211	120
101.	H(58)-C(8)-C(9)	119.889	120	129.	C(15)-C(13)-C(11)	115.694	117.6
102.	C(10)-C(8)-C(9)	117.869		130.	C(12)-C(13)-C(11)	114.4	120
103.	H(59)-C(9)-C(11)	119.76	120	131.	N(7)-C(15)-O(16)	110.406	122.6
104.	H(59)-C(9)-C(8)	120.857	120	132.	N(7)-C(15)-C(13)	108.406	112.74
105.	C(11)-C(9)-C(8)	119.297		133.	O(16)-C(15)-C(13)	141.156	123
106.	C(14)-C(12)-C(13)	121.414	117.6	134.	H(57)-N(7)-C(15)	118.365	117.4
107.	C(14)-C(12)-C(10)	116.83	117.6	135.	H(57)-N(7)-C(6)	117.17	118
108.	C(13)-C(12)-C(10)	121.444	120	136.	C(15)-N(7)-C(6)	124.436	
109.	H(61)-C(11)-C(13)	122.456	120	137.	H(56)-C(6)-H(55)	109.032	109.4
110.	H(61)-C(11)-C(9)	112.678	120	138.	H(56)-C(6)-N(7)	108.38	
111.	C(13)-C(11)-C(9)	124.85		139.	H(56)-C(6)-C(4)	109.961	109.41
112.	Cl(51)-Ni(49)-Cl(50)	96.685		140.	H(55)-C(6)-N(7)	114.898	
113.	Cl(51)-Ni(49)-O(16)	63.813		141.	H(55)-C(6)-C(4)	107.537	109.41
114.	Cl(51)-Ni(49)-O(17)	153.491		142.	N(7)-C(6)-C(4)	106.966	
115.	Cl(51)-Ni(49)-O(40)	105.03		143.	H(54)-C(5)-C(4)	127.624	120

116.	Cl(51)-Ni(49)-O(41)	131.268		144.	H(54)-C(5)-C(3)	127.878	120
117.	Cl(50)-Ni(49)-O(16)	143.639		145.	C(4)-C(5)-C(3)	104.498	
118.	Cl(50)-Ni(49)-O(17)	104.229		146.	O(1)-C(4)-C(5)	111.146	120
119.	Cl(50)-Ni(49)-O(40)	142.845		147.	O(1)-C(4)-C(6)	123.523	120
120.	Cl(50)-Ni(49)-O(41)	70.678		148.	C(5)-C(4)-C(6)	125.319	121.4
121.	O(16)-Ni(49)-O(17)	89.789		149.	H(53)-C(3)-C(5)	128.043	120
122.	O(16)-Ni(49)-O(40)	73.516		150.	H(53)-C(3)-C(2)	127.92	120
123.	O(16)-Ni(49)-O(41)	145.438		151.	C(5)-C(3)-C(2)	104.036	
124.	O(17)-Ni(49)-O(40)	66.948		152.	H(52)-C(2)-O(1)	117.352	108
125.	O(17)-Ni(49)-O(41)	72.154		153.	H(52)-C(2)-C(3)	130.901	120
126.	O(40)-Ni(49)-O(41)	72.328		154.	O(1)-C(2)-C(3)	111.747	118.1
127.	Ni(49)-O(16)-C(15)	111.338		155.	C(2)-O(1)-C(4)	108.571	113.95
128.	C(15)-C(13)-C(12)	129.901	117.6				

3.8. Antimicrobial Activity

The *in vitro* antimicrobial activity of the synthesized ligand and its metal(II) complexes was performed on the selected bacteria Gram-positive bacteria (*Staphylococcus aureus*, *Streptococcus pyogenes*), Gram-negative bacteria (*Escherichia coli*, *Klebsiella pneumoniae*) and different fungal *Candida albicans*, *Candida glabrata*, *Candida tropicalis* and *Candida krusei*. All of the synthesized compounds illustrated excellent biological activity against all the tested microorganisms. A comparative examinations of the ligand and its Ni(II) and Co(II) metal complexes designated that the metal complexes show higher antimicrobial activity than the synthesised ligand. It is eminent that coordination boosts the ligand to perform as an effective and significant bactericidal and fungicidal agents by inhibiting the growth of bacteria and fungi respectively, therefore inhibition zone of Ni(II) and Co(II) metal complexes was found to be higher as compared to their free ligand [Figure 5 (a) and (b)].

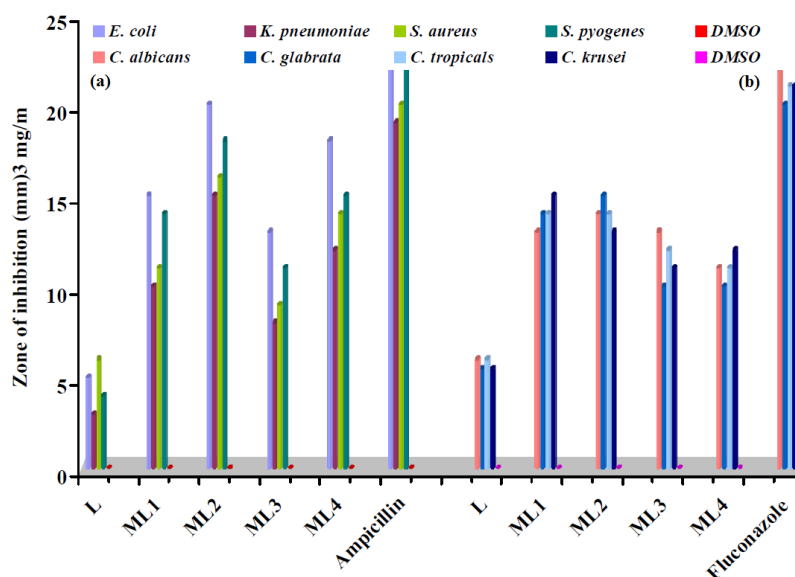


Figure 5. (a) Bacterial growth inhibition in millimeters (mm) for different compounds. Ampicillin used as reference compound. (b) Fungal growth inhibition in millimeters (mm) for different compounds. Fluconazole used as reference compound

The high antimicrobial activity of Ni(II) and Co(II) metal complexes was most likely because of the greater lipophilic nature of these complex. The improvement in the antimicrobial activity of the metal complexes as compared to the synthesized free ligand can be explained on the basis of chelation theory and Overtone’s concept [55,56]. The overtone’s concept of cell permeability reveals that the lipid membrane which is present around the cell supports the passage of only lipid soluble material, because of that liposolubility was believed to be the most significant factor involved in the control of antimicrobial activity. In the chelation process, the metal ion polarity will be reduced to a greater extent as a result of the overlap of the ligand orbital and partial sharing of positive charge of metal ion with donor groups [57,58]. In addition, the lipophilicity of the complex is improved by the increased delocalization of the π -electrons over the entire chelate ring. As a result, the increased lipophilicity enhances the infiltration of the synthesized complexes into the lipid membrane and therefore, the metal binding site on enzymes of microorganisms are blocked [59]. In addition, the synthesized metal complexes also perturb the cell respiration process that restricts the synthesis of the proteins which in turn blocks the further growth of these microorganisms [60]. There are other factors which also increase the activity are solubility, conductivity and bond length between the metal and ligand [61-64]. The MIC of the newly synthesized ligand and its Ni(II) and Co(II) metal complexes are shown in Figure 6(a) and (b). It is clear from the experimental results that the MIC values observed designate that the metal(II) complexes have higher antimicrobial activity than the free ligand (L).

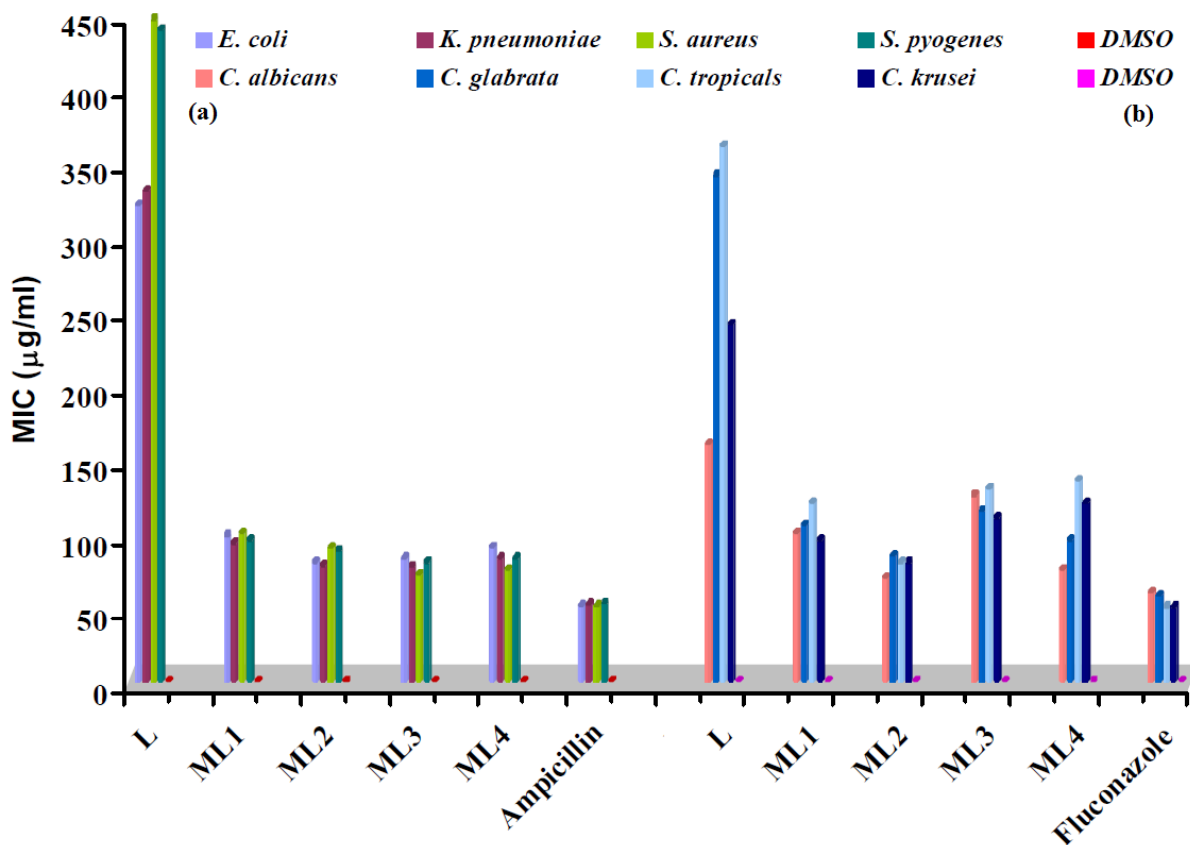


Figure 6. Minimum Inhibitory Concentrations (MIC) of ligand and its metal complexes against different (a) Bacterial species and (b) Fungal species

3.9. Antioxidant assay (DPPH free radical scavenging activity)

The newly synthesized ligand and its metal complexes were screened for hydrogen donating or free radical scavenging activity by UV-*vis* spectrophotometer using the stable DPPH method [65]. The DPPH radical is one of the most commonly used substrates for fast evaluation of antioxidant activity because of its stability and simplicity of the assay. The embodiment of various metal ions in to the ligand validates broad-spectrum results. In the present investigation Ni(II) and Co(II) metal complexes exhibits good and moderate scavenging activity respectively. However, it has been observed that the metal complexes exhibited higher scavenging activity than the synthesised ligand. In addition it was observed that the synthesized ligand and its metal complexes scavenged the DPPH radical in a concentration dependent manner and therefore on increasing the concentration of the tested compounds, the scavenging activity was increased. DPPH antioxidant assay is based on capability of decolourization of a stable free radical DPPH in the presence of antioxidants. Results of percentage of free radical scavenging activity are shown in Fig. 7.

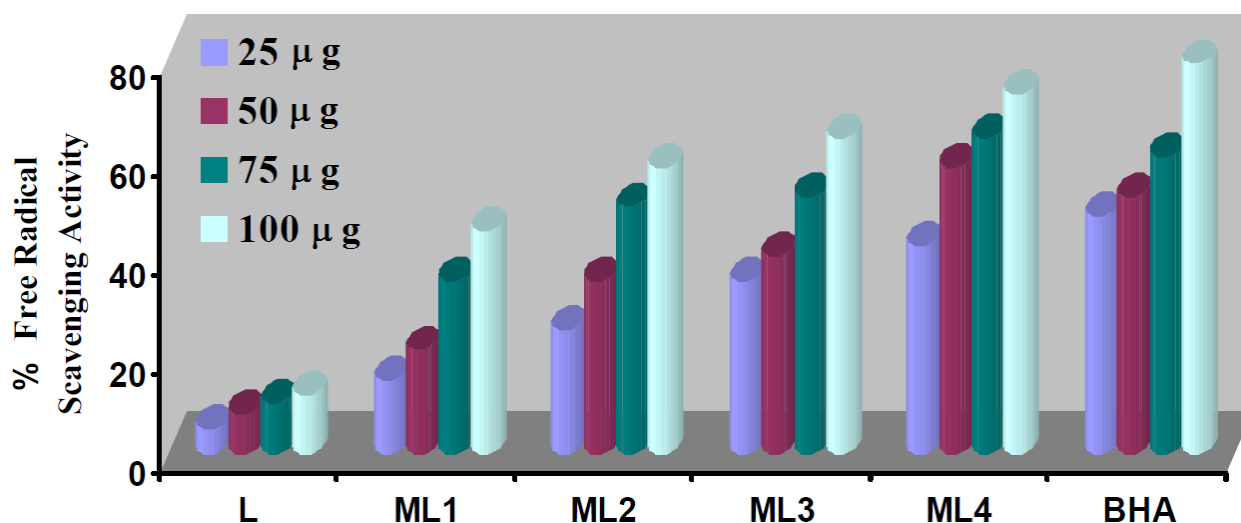


Figure 7. Antioxidant activity results of ligand (L) and its metal complexes

In DPPH assay, the ligand and its complexes act as donors of hydrogen atoms or electrons in transformation of DPPH radical into its reduced form DPPH-H. When DPPH accepts an electron donated by an antioxidant compound, the DPPH is decolorized which can be quantitatively measured by changes in absorbance. Lower absorbance values of the reaction mixture indicated higher free radical scavenging activity. The radical scavenging activity of the compound depends on the structural factors such as the phenolic hydroxyl, carboxylic groups and other structural features [66].

4. CONCLUSIONS

In this study, we synthesized N,N'-bis(furan-2-ylmethyl)benzene-1,2-dicarboxamide, ligand and its Co(II), Ni(II) metal complexes. The synthesized ligand and metal complexes were

characterized by using various characterization techniques. The Job's method was adopted to validate the stoichiometric composition of the complexes. On the basis of spectroscopic results, an octahedral geometry for metal complexes has been assigned. The antimicrobial activity results indicated that all metal complexes have been found to be more effective than its ligand as the process of chelation dominantly affects the overall biological behavior of the compounds. All compounds showed varying antioxidant (free radical scavenging) activities when compared to the standard. Complexation enhanced the efficacy of the all the compounds, which was attributed to the increase in lipophilicity on metallation. Semiconducting nature of the metal complexes was observed by conductivity measurements. Consequently from all these widespread examinations, it was concluded that the synthesized compounds offered a significant, resourceful and important information of coordination compounds of its kind and also they could be used as effective biological agents with advanced efficiency.

ACKNOWLEDGEMENTS

This project was funded by the Deanship of Scientific Research (DSR), King Abdulaziz University, Jeddah, under grant No. 407-130-1436-G. The authors, therefore, acknowledge with thanks DSR technical and financial support.

References

1. M.S. Refat, M.Y. El-Sayed, A.M.A. Adam, *J. Mol. Struct.* 1038 (2013) 62–72.
2. A.A. Nejo, G.A. Kolawole, A.O. Nejo, *J. Coord. Chem.* 63 (2010) 4398–4410.
3. D.C. Crans, K.A. Woll, K. Prusinskas, M.D. Johnson, E. Norkus, *Inorg. Chem.* 52 (2013) 12262–12275.
4. W. Rehman, F. Saman, I. Ahmad, *Russ. J. Coord. Chem.* 34 (2008) 678–682.
5. A. Choudharya, R. Sharma, M. Nagar, *Int. Res. J. Pharm. Pharmacol.* 1 (2011) 172–187.
6. S.P. Fricker, *Dalton Trans.* 43 (2007) 4903–4917.
7. R.R. Crichton, D.T. Dexter, R.J. Ward, *Coord. Chem. Rev.* 252 (2008) 1189–1199.
8. R. Cini, G. Tamasi, S. Defazio, M.B. Hursthouse, *J. Inorg. Biochem.* 101 (2007) 1140–1152.
9. M. Sonmez, A. Levent, M. Sekerci, *Russ. J. Coord. Chem.* 30 (2004) 655–659.
10. H.L. Singh, M. Sharma, A.K. Varshney, *Synth. React. Inorg. Met.-Org. Chem.* 30 (2000) 445–456.
11. Z.H. Chohan, M. Praveen, A. Ghaffer, *Synth. React. Inorg. Met.-Org. Chem.* 28 (1998) 1673–1687.
12. S. Adsule, V. Barve, D. Chen F. Ahmed, Q.P. Dou, S. Padhye, F.H. Sarkar, *J. Med. Chem.* 49 (2006) 7242–7246.
13. S. Tardito, O. Bussolati, M. Mattini, M. Tegoni, M. Giannetto, V.D. Asta, R. Franchi-Gazzola, M. Lanfranchi, M.A. Pellinghelli, C. Mucchino, G. Mori, L. Marchio, *J. Med. Chem.* 50 (2007) 1916–1924.
14. S. Chandra, D. Jain, A.K. Sharma, P. Sharma, *Molecules*, 14 (2009) 174–190.
15. M. Geraghty, V. Sheridan, M. McCann, M. Devereux, M. McKee, *Polyhedron*. 18 (1999) 2931–2939.
16. S. Chandra, A.K. Sharma, *J. Coord. Chem.* 62 (2009) 3688–3700.
17. M. Geraghty, V. Sheridan, M. McCann, M. Devereux, V. McKee, *Polyhedron*. 18 (1999) 2931–2939.
18. M.C. Rodríguez-Argüelles, P. Tourón-Touceda, R. Cao, A.M. García-Deibe, P. Pelagatti, C. Pelizzi, F. Zani, *J. Inorg. Biochem.* 103 (2009) 35–42.

19. S. Chandra, L.K. Gupta, *Spectrochim. Acta-A*. 60 (2004) 3079- 3085.
20. J.K. Swearingen, D.X. *Trans. Met. Chem.* 25 (2000) 241-246.
21. S. Chandra, L.K. Gupta, *Spectrochim. Acta-A*. 60 (2004) 1751-1761
22. S. Chandra, L.K. Gupta, *Spectrochim. Acta-A*. 60 (2004) 2767-2774.
23. R.A. Shiekh, M.A. Malik, S.A. Al-Thabaiti, M.Y. Wani, A. Nabi, *The Scientific World Journal*, 2014 (2014) 1-9.
24. S.A. Khan, A.M. Asiri, K. Al-Amry, M.A. Malik, *The Scientific World Journal*, 2014 (2014) 1-9.
25. M. Sheble, S.M.E. Khalil, F.S. Al-Gohani, *J. Molc. Struct.* 980 (2010) 78-87.
26. S. Chandra, L.K. Gupta, *Spectrochim. Acta A*, 61 (2005) 269-275.
27. Chen. Xiang, Tang. Li-Jun, Sun. Yu-Na, Qiu. Pei-Hong, L Guang, *Jol. Inorg. Biochem.* 104 (2010) 379–384.
28. Qu. Jian-Qiang, Qu. Ling, Yang. Qiu-Hu, W. Liu-Fang, *Chemical Papers*, 63 (2009)426–431.
29. M. Hong, Yin. Han-Dong, Li. Wen-Kuan, Y. Xi-Ying, *Inorg. Chem. Commun.* 14 (2011) 1616-1621.
30. A.A. Khandar, R.J. Butcher, M. Abedi, S.A. Hosseini-Yazdi, M. Akkurt, M.N. Tahir, *Polyhedron*. 29 (2010)3178-3182.
31. A.A.A. Emara, A.A. Abu-Hussen, *Spectrochim. Acta Part A*. 64 (2006) 1010-1024.
32. M.Z. David, R.S. Daum, *Clin. Microbio. Rev.* 23(3) (2010) 616–687.
33. H. de Lencastre, D. Oliveira, A. *Current Opinion in Microbiology*, 10(5) (2007) 428–435.
34. L. Zhang, D. Pornpattananangkul, J, Hu C.-M. C.-M, Huang, *Current Medicinal Chemistry*, 17 (6) (2010) 585–594.
35. S.V. Jovanovic, S. Steenken, M. Tomic, B. Marjanovic, M.G. Simic, *J. Am. Chem. Soc.* 116 (1994) 4846-4851.
36. R. Amarowicz, R.B. Pegg, P.R. Moghaddam, B. Barl, J.A. Weil, *Food Chem.* 84 (2004) 551–562.
37. R.M. Silverstein, F.X. Webster, *Spectroscopic Identification of organic Compounds, 6th Edn, John Wiley and Sons. Inc. New York* 482 (1998).
38. W. Kemp, *Organic Spectroscopy, Macmillan Press Ltd.* (1975).
39. K. Snakeroot, *Infrared spectra of Inorganic and Coordination Compounds, Wiley Internscience, New York*, 90 (1970).
40. R.A. Sheikh, S. Shreaz, G.S. Sharma, A.K. Luqman A.H. Athar, *J. Saudi Chem. Soc.* 16 (2012) 353-361.
41. P.S. Kalsi, *Spectroscopy of organic compounds, fourth ed., New Age International (P) Ltd., New Delhi*, (1999).
42. S.C. Rawle, C.P. Moore, N.W. Alcock, *J. Chem. Soc. Dalton Trans.* (1992) 2755-2757.
43. R.A. Sheikh, S. Shreaz, M.A. Malik, A.K. Luqman A.H. Athar, *J. Chem. Pharm. Res.* 2 (2010) 133-146.
44. M. Mann, *Organic Mass spectrometry.* 25 (1990) 575-587.
45. R.A. Sheikh, M.Y. Wani, S. Shreaz, A.A. *Arabian J. Chem.* 10.1016/j.arabjc.2011.08.003
46. A.A.A. Emara, O.M.I. Adly, *Transition Met. Chem.* 32 (2007) 889-901.
47. A.C. Gaillot, B. Lanson, V.A. Drits, *Chem. Mater.* 17 (2005) 2959-2975.
48. M.A. Cheney, P.K. Bhowmik, S. Qian, S. W. Joo, W. Hou, J. M. Okoh. *J. Nanomaterials* (2008) 1-8.
49. S. Chandra, L.K. Gupta, *Spectrochimica Acta A*. 61 (2005) 1181-1188.
50. S. Chandra, L.K. Gupta, *Spectrochimica Acta A*. 60 (2004) 767-2774.
51. S. Chandra, L.K. Gupta, *Spectrochimica Acta A*. 60 (2004) 3079-3085.
52. M.S. Refat, I.M. El-Deen, M.A. Zein, A.M.A. Adam, M.I. Kobeasy, *Int. J. Electrochem. Sci.*, 8 (2013) 9894 - 9917
53. R.C. Maurya, S. Rajput, *J. Mol. Struct.* 687 (2004) 35-44.
54. R.C. Maurya, S. Rajput, *J. Mol. Struct.* 833 (2007) 133-144.

55. Z.H. Chohan, M. Arif, M.A. Akhtar, C.T. Supuran, *Bioinorg. Chem. Appl.* 2006 (2006) 1–13.
56. K.N. Thimmaiah, W.D. Liyod, G.T. Chandrappa, *Inorg. Chim. Acta.* 106 (1985) 81–83.
57. K. Kralova, K. Kwassova, O. Svajlenova, J. Vanco, *Chem. Pap.* 58 (2000) 357-361.
58. J. Pwerekh, P. Inamdhar, R. Nair, S. Baluja, S. Chand, *J. Serb. Chem. Soc.* 70 (2005) 1155-1161.
59. Y. Vaghasia, R. Nair, M. Soni, S. Baluja, S. Chand, *J. Serb. Chem. Soc.* 69 (2004) 991-998.
60. N. Raman, *Res. J. Chem. Environ.* 4 (2005) 1-9.
61. Z.H. Chohan, H. Pervez, A. Rauf, K.M. Khan, C.T. Supuran, *J. Enzym. Inhib. Med. Chem.* 39 (2004) 417-423.
62. V.P. Singh, A. Katiyar, S. Singh, *Biometals.* 21 (2008) 491-501.
63. Z.H. Chohan, A. Munawar, C.T. Supuran, *Metal Based Drugs*, 8 (2001) 137-143.
64. B.G. Tweedy, *Phytopathology*, 55 (1964) 910-914.
65. R.P. Singh, K.N.C. Murthy, G.K. Jayaprakasha, *J. Agr. Food Chem.* 50 (2002) 81-86.
66. M.A.R. Bhuiyan, M.Z. Hoque, S.J. Hossain, *World J. Agr. Sci.* 5 (2009) 318–322.

© 2016 The Authors. Published by ESG (www.electrochemsci.org). This article is an open access article distributed under the terms and conditions of the Creative Commons Attribution license (<http://creativecommons.org/licenses/by/4.0/>).